Translation of Mainz Geoscientific Report 26 Pages 131-184 15 Figures 12 Tables Mainz, December, 1997

Geological, petrographic, geochemical and petrophysical investigations on roofing slates

WOLFGANG WAGNER & HORST BAUMANN & JÖRG F. W. NEGENDANK & FRANK ROSCHIG

Abstract: Slate is one of the most durable natural roofing materials. Geological and petrographical investigations are traditionally given more importance in the appropriate German standards, in contrast to foreign standards. Within the scope of the research presented in this document, fundamental inferences regarding the material quality of slate as obtained within this research project are to be presented and, if possible, incorporated into a single European standard (EN 12326-1 and (EN 12326-2)

In order to reduce the natural variation found within the investigated deposits, whole blocks were taken as random samples from seven sites and split immediately in order to obtain homogeneous tiles for the purpose of the investigation. The sampling encompassed Lower Devonian and Middle Devonian German slates as well as Ordovician and Lower Cambrian Spanish slates.

A survey on European slate occurrences and their tectonostratigraphic groupings is given. Particular emphasis is placed on the geological development of roofing slate occurrences from the Rhineland-Palatinate area, explained in newer plate-tectonic models.

In the petrographic investigations, the methods of DIN 52 201 were expanded upon and new methods were developed. The quality of the slates is determined by the quality of the structure and, if present, by the content of the available detrimental constituents. In addition to a quality assessment, petrographical analysis provides the possibility of determining the provenance of the slate.

Chemical analyses were made not only of specimens from the seven main extraction areas, but also for virtually all German (including old deposits), European and some non-European roofing slates. These chemical tests display a large degree of similarity despite the varying provenances of the slates.

Nevertheless, some peculiarities are recorded which are particular to occurrences from specific regions and which also indicate provenance variations between Spanish and German slates. As an example, a trace element analysis on a series of German and Spanish slates showed differences between the two in their lead and nickel content.

Within the scope of the petrophysical investigations, the existent methods which are utilised for the investigation of slate in Germany were critically evaluated (DIN 52 102, DIN 52 103, DIN 52 104, DIN 52 112, DIN 52 201, DIN 52 204, and DIN 52 206).

In the case of the bending strength, only the breaking strength was used for comparative purposes. The conversion factor for bending strength normally used for natural rock cannot be applied for slate because it results in atypical values due to the anisotropy of the slate. To compensate, the breaking strenght values were normalized to 1 mm thickness which facilitated comparability.

Furthermore, it became apparent that the definition, “air-dry” is too imprecise. However, for a better reproducibility, only dried (at 110°C) samples or water-saturated samples were used.

The ultrasound compression wave velocity in the direction of the cleavage was determined using a measuring instrument which was specifically developed by the research team. However, the slate samples still showed clear anisotropy whilst the maximum lay in parallel with the strike of the cleavage/stratification (provided that a clear layering was present).

The reduction in durability through stress tests such as the acid test, the thermal cycle test and the freeze-thaw test can be particularly well measured using compression wave velocity. It can very well be compared with the drop of the bending strength after identical tests.

In a long-term acid test, the time-span of the normal acid test (twenty-eight days) was extended to over 2000 days. By means of this test, it was observed that carbonate-free, qualitatively good samples displayed few changes and absolutely no structural damage even over such a long time period. Carbonate-rich slates, on the other hand, can display a mass increases of more than 50 %. In the case of asbestos cement tiles (as a means of comparison) asbestos fibres released themselves from the structure after 500 days, although there was no structural damage.

Meanwhile, the summary of the results could be incorporated into a new European slate standard, for example, the petrographic analysis and details on the Bending test.

1. Introduction

1.1 Project, task assignment

The utilisation of slate has increased in the last ten years. As a result, questions associated with this subject regarding the quality of slate have once again arisen. This natural product has the reputation of being one of the most durable roofing materials available. There exist roofing slates which are over 250 years old and still in good functioning condition.

When assessing the quality of slates, geological and petrographic methods are traditionally given more importance (for example, when elaborating the DIN 52 201 around 1993). The aim of the present investigation was to take this into account along with new findings for the creation of a new European standard (for example, in the compilation of the new DIN prEN 12326, Parts 1 and 2). Fundamental findings in relation to this aim were

to be realised within the parameters of a single research project with contributions from the fields of geology of mineral deposits, petrography, geochemistry and petrophysics. In addition, the traditionally applied technical methods (DIN 52 201) were compared with more modern methods from the areas of petrography and petrophysics.

The additional aim of the project was the scientific compilation of basic research guidelines for the investigation of deposits and the qualities of roofing slates as a precondition for the optimization of the production and for the purpose of quality control within the industry.

1.2 Acknowledgements

The work presented herein was undertaken over a period of three years as a project within the framework of the programme ”Wirtschaftsnahe Forschung” (Economy-related research) which was supported by the Ministry for the Economy, Traffic, Agriculture and Wine Growing of Rhineland-Palatinate. The title of the research project was ”Geology of mineral deposits, quality control and the utilisation of roofing slate”. The scientific workgroup consisted of the attributed authors of this report. The project management lay under the responsibility of Prof. Dr. J.F.W. Negendank and Dr. W. Wagner.

The investigations took place in the laboratories of the Department of Geology at the University of Trier. In addition, the Project received considerable assistance and support from the firms, Rathscheck Schiefer and Dach-Systeme KG, Mayen, in the areas of previous research materials, travel costs and survey work.

Furthermore, the companies Johann & Backes OHG, Bundenbach, Nikl. Theis Nachf. Boeger Schieferwerk GmbH, Bundenbach, and Magog Schiefergruben GmbH & Co. KG, Fredeburg, provided the authors with slate samples and also assisted in the time consuming processes of sample preparation.

We would like to thank all of those involved in this project.

1.3 Quality control of slates

At this point, we would like to define this line of investigation:

There are four different areas involved in the assessment of the quality of a slate sample (HOPPEN 1987). These are:

- Material properties (deposit situation, rock constituents, etc.)
- Procurement and processing (extraction, special regulations, quality control)
- Placement (roof types, fastening, supportive structure)
- Location and Exposition (location of the house in lowland, middle elevation, high elevation; on the coast or inland; on the countryside or in an industrial area; exposition of the roof on the sun-facing or non-sun-facing side).

In general, the investigations described in this report make statements regarding the quality-level of the material and also, partially, on the processing. For the

analysis/judgement of these two aspects, the following considerations ought to be taken into account:

On the average, 10 to 15 % of the total excavated mass of slate (open-cast mining, 1 - 5 %, open-cast mining with saws approx. 10 %) can be utilised for roofing slate. When investigating roof slate tiles from one particular load, it must be taken into account that the slate may derive from different geological deposits which may show variations. In addition, it must be noted that in a slate which shows a recognizable angle between cleavage and stratification, there are often less variations to be found as compared to a roof slate where cleavage and stratification are in parallel. Thus, a low strength silt deposit can appear as a slate tile with characteristics which are completely different to a slate tile derived from a previously overlying and/or underlying clay layer. When looking at a deposit area which shows an angle between cleavage and stratification and which also possesses a change from clay to silt, the slate of the deposit displays homogeneous characteristics due to the cleavage process and thus the "close mingling" of the silt and clay particles; then the variations are smaller.

When analysing roof slates from one bundle, the following situation must be taken into account. In a deposit of predominantly high quality and rarely occurring bad material quality a lack of selection could result in a load of low quality, whereas a deposit of a consistently average quality could reach the same standard as the former as a result of a high selection (comp. WAGNER 1992). The investigated tiles thus do not make definitive statements as to the overall quality of the deposit.

1.4 Sampling

In the investigation of a slate deposit, which also displays variations, it is not possible to investigate the cross-section or longitudinal section millimetre by millimetre. The sampling areas are mostly small and also limited to deposits taken from the extraction area. Thus, it is necessary to take samples which are representative.

Within the scope of this work, whole blocks were removed as random samples and split in order to provide enough tiles for petrophysical, geochemical, and petrographic investigation. The tiles were acquired from a single homogenous-appearing deposit (cf. Chapter 4.4).

The following table indicates from which occurrences the samples were taken:

	Age	Name of formation/Location
I	Lower Devonian (Siegenian?)	Mayener Dachschieferfolge (Mayen roofing slate sequence) East Eifel, Rhineland-Palatinate (cf. fig. 2, no. 4; fig. 4)
II	Lower Devonian (Lower Emsian)	Hunsrück shales s. str., Hunsrück NW edge, Rhineland-Palatinate (cf. fig. 4)
III	Lower Devonian (Lower Emsian)	Hunsrück shales s. str., Central Hunsrück, Rhineland-Palatinate (cf. fig. 4)
IV	Middle Devonian (Eifelian)	Fredeburg beds, East Sauerland, Northrhine-Westphalia (cf. fig. 2, no. 10; Fig. 4)
V	Middle Devonian (Eifelian)	Fredeburg beds, East Sauerland, Northrhine-Westphalia (cf. fig. 2, no. 10)
VI	Ordovician (Caradocian-Ashgillian)	Middle Argüeira formation, La Cabrera, Province León, Spain (cf. fig. 2, no. 1, and fig. 3, no. 2)
VII	Lower Cambrian	Cadana formation, A Terra Cha, Province Lugo, Spain (cf. fig. 2, no. 1, and fig. 3, no. 4)

Sample VI was deliberately extracted from a surface close area where the technical characteristics remain imperfect. Sample VII is a phyllitic chlorite slate.

In addition to these large random samples used for all investigations, additional samples were taken for individual investigations for the purpose of comparison. Thus the results of these experiments cannot be compared in all characteristics with the results of the investigated tiles since the former encompass a defined part by volume (approx. ¼ m^3) of the deposit (random sample) whilst the slabs extracted from a load are more than likely representative for a whole layer or the entire area within which extraction took place.

1.5 Geological and/or tectonostratigraphic patterns of European roofing slates

Except for two occurrences (the slate occurrence in the Pyrenees, fig. 2, no. 14, and slate occurrences in Liguria, Italy, fig. 2, no. 9), all European slate occurrences date from the Palaeozoic. Although most of them are argillaceous slates with a similar sedimentation history (cf. Chapter 1.6) and are furthermore ”very-low-grade” metamorphic

rocks of a pressure-emphasized metamorphosis, they originate from different tectonostratigraphic units.

Modern plate-tectonic views of the European Variscides, within which most slate occurrences are found, consider this as a puzzle consisting of different continental microplates (terranes) which were subsequently fitted together into the later orogen (cf. FRANKE & MEISCHNER & ONCKEN 1996 and FRANKE & DALLMEYER & WEBER 1995).

According to palaeo-magnetic findings, the drift history of the northward orientated Avalonia begins during the Ordovician with the separation of Amorica and Gondwana. Until the Silurian, this micro-continent had generally followed the path of Baltica (more or less the region of present-day Scandinavia). This microcontinent was followed, also in a northerly direction, by the microcontinent of Amorica and approached the southern Avalonian edge of the Old Red continent during the late Ordovician up to the early Lower Devonian. The Old Red continent was made up of Avalonia, Baltica, and Laurentia which had fused together. The slate occurrences of North Wales (for example, Penrhyn; fig. 2, no. 2), which had been folded during the Caledonian orogenesis and the occurrences in northern Norway (cf. fig. 2, no. 11) also belong to this continent.

From the late Lower Devonian onwards, a new basin formed roughly along the old suture zone of Avalonia and Amorica the extension of which resulted in the formation of the Rheno-Hercynian Ocean. The Martelange slate deposits in Belgium and Luxembourg (fig. 2, no. 5) and possibly also the Moravian slate deposit (Moravosilesium; cf. fig. 2, no. 8; cf. WAGNER & STANEK 1991), specimens I, II and III belong to the Rheno-Hercynian zone of the Variscides that formed the southern shelf of the Old Red Continent. Their folding was caused by the collision of a terrane (the so-called Central German Ridge) with the northern continent in the course of the Upper Carboniferous.

Southern Saxothuringia, as a part of Amorica, includes the Thuringian slate occurrences (fig. 2, no. 7). Moreover, the central and north Amorican massif with the slate occurrences in Mael Charhaix (Brittany) also belong to with the former.

The large Spanish deposits (cf. fig. 2, no. 1, and 12, fig. 3) and those of Portugal (fig.2, no. 6) form part of the Central Iberian zone.

European roofing slates, even with their similarities in mineralology and geology, still have a different genesis and tectonostratigraphic alignment.

1.6 Geological formation of roofing slates

Roofing slates can easily be split and are very resistant to weathering. They consist of argillaceous clay and silt slates with a very strong slaty cleavage due to compression, folding, and a very low pressure-related metamorphosis. In addition to these pure argillaceous slates, there are also roofing slates with a higher carbonate content (therefore called ”carbonate slates” acc. to DIN prEN 12 326) or phyllitic slates with a slightly higher level of metamorphism which can also be used as roofing slates.

The formation of a roofing slate deposit occurs only in special sedimentation areas with particularly fine granular sedimentation. Mostly, this formation occurs either under

deep marine conditions or distal to the supply area so that deposits of coarser particles are comparatively rare. As far as the Mayen (Moselschiefer) roofing slates and the Hunsrück slates are concerned, rarely occurring sand and silt deposits are probably tempestites, i.e. the results of storm floods which took place at the distant coast.

The creation of a roofing slate deposit will be explained here using roofing slates from Rhineland-Palatinate (East Eifel and Hunsrück). DITTMAR (1996) employed a modern plate tectonic approach using observations made by FRANKE and ONCKEN (1990). This approach indirectly explains the formation of roofing slates:

The oldest deposit of clay slate with the ability to metamorphose into argillaceous slate occurred in the Mayen area in the so-called ”Moselgraben” (sample I) during the Siegenian, already. It was only in the Lower Emsian that argillaceous slate could form in the Altlay area (sample II) and in the central Hunsrück area (sample III). This basin formation was probably caused by extension of the continental crust. At the same time, the opening of the Lizard-Giessen-Ostharz Ocean, south of the present-day Rhenish Massif, occurred. In the Upper Devonian, a subduction of the oceanic crust in south-east direction occurred on the southern edge of the ocean so that an active plate boundary was created. The deeper parts of this previous continental margin area are preserved today in the Middle German Crystalline Ridge. Turbidites were deposited on the active plate boundary (Giessener greywackes). In the upper Lower Carboniferous, this southern microcontinent (the so-called Middle German Ridge) collided with the Rheno-Hercynian basin located north of it. As a result, the oceanic crust was subducted with the consequence that it is no longer possible to locate remnants of the ocean in the East Eifel-Hunsrück area. The collision influenced the folding of the sediments of the Rheno-Hercynian area until the Upper Carboniferous. DITTMAR assumes that the sedimentary sequence was sliced off from their continental base and thus formed several nappe units, such as the Hunsrück nappe and the imbricate fan of the Mosel, which lies north of the former. According to the most recent findings of contemporary roofing slate excavation (WAGNER & HOPPEN 1995), this imbricate fan is considerably more imbricated than previously thought.

However, these tectonic structures only belong to the lower section of an entire nappe pile and/or a widespread duplex structure, which may have originally contained a further nappe system (Lizard-Giessen-Harz nappe) with the typical sedimentation of the Giessen greywacke and perhaps parts of the ocean floor. Meanwhile, however, this upper nappe system in the western section of the Rhenish Massif has almost completely eroded, thus leaving relatively deep-lying parts of the orogen. In any case, it is still possible to infer the previous tectonic superimposition from the grade of metamorphosis of the rocks and thus also of the roofing slate.

Fig. 4 shows the various stages of this development, although the lower section (orogenic final phase) of the diagram does not display a definite time period, but rather the estimated geometry of the mountain area before the beginning of the late orogenic extension and the later erosion.

2. Petrographic investigations

For the petrographic investigations orientated thin sections were used for the determination of the transparent mineral content as well as polished sections for the analysis of

the ore phase. The orientation of the thin sections facilitated the determination of the angle of cleavage and stratification plane with the microscope. In addition to the mineral-specific analyses, the number of mica layers per millimetre and the structural formation of the slate was determined as a qualitative and regionally associated characteristic of the extraction zone.

The petrographic analysis with thin sections and polished sections showed that an exact characterization of any slate is possible. The mineral association and the determination of the structural characteristics in the thin sections and polished sections allow the determination of the type of deposit and thus its origin. Thus, it is possible for the first time to specify the origin of roofing slates (the investigation is made at best with a number of slate tiles, although it may be possible to make an identification with a single tile if certain characteristics, highly typical of a region, are present). The investigation consists of a combination of a thin section examination (using a polarisation microscope) and a polished section examination (using reflected light in the microscope). In the thin sections, it is possible to determine the porphyroblasts and thus the quantity of carbonate and organic substances and to infer how these are incorporated in the slate (see table 1). Using petrographic techniques, it is thus possible to determine whether the slate consists of pure argillaceous slate, argillaceous slate with silt lenses or silty slate. In addition, the angle between cleavage and stratification can be determined.

The opaque components are finely disseminated graphite as well as ore minerals. The ores, which occur both regularly and irregularly in the porphyroblasts and also as raw ore have sizes varying between more than 1 mm down to pigment size. The quantity measured as percentage by volume ranges between less than 1 % to over 7 %. The individual opaque phases are best suited to determine the provenance.

- Pyrite FeS_2 (cubic): cubic, spherical, pigment-like, framboids of various sizes, framboid clusters, partially arrayed in a pearl chain formation, pyrite layers in parallel with the cleavage.
Pyrites are typical for German slates, such as the framboids in sample I, or other slates from the East Eifel region, and the cubic pyrites in sample II, whilst pyrites are less frequent in Spanish slates (for example, sample VI).

- Marcasite FeS_2 (orthorhombic): Does not occur at all in German slates (samples I to V). Does, however, appear in Spanish slates (for example, sample VI) in addition to pyrrhotite.

- Pyrrhotite $Fe_{1-x}S_x$ - Occurs in large crystals and layers in parallel with the cleavage, partly combined with chalcopyrite. Totally absent in German slates (samples I to V) and typical for Spanish slates, which show a higher level of metamorphosis (temperature).

- Chalcopyrite $CuFeS_2$ - Associated with pyrrhotite and pyrite. Typical in Spanish slates, for example, sample VI, though in minor quantities, only.

- Ilmenites $FeTiO_3$ only appear in the form of small fragments in German slates. However, in Spanish slates from Galicia and León, they form large porphyroblasts, which are partially transformed into leucoxenes. The contour shapes indicate sprouting during higher degrees of metamorphosis.

- Leucoxenes - as Ilmenite

- Titanomagnetite C1 - C7 (deuteric oxidation levels and hydrothermal/low temperature oxidation phases with maghemite, haematite and titanite): very rare. Occurs in slates from Penryhn, North Wales.

- Limonite: rare (a mixture of Goethite and Lepidocrocite)

In the polished sections, the ore minerals which can be recognized are primarily pyrite and its numerous forms, ilmenite, leucoxenes, pyrrhotite, marcasite and sometimes also copper pyrite.

The German slate samples, samples I to V, possess primarily pyrites and small ilmenites due to their lower level of metamorphosis, whereas the majority of the Spanish slates show large ilmenites/leucoxenes and pyrrhotites due to their higher degree of metamorphosis. Sample I can be clearly distinguished from samples II and III by its pigment-like pyritic framboids that are present therein. Sample II, on the other hand, can be distinguished by small quadratic pyrites.

The microstructure can be observed in thin sections or in a fractue plane through the scanning electron microscope.

The orientation and thickness of the mica layers is variable and can be described using methods developed by WAGNER (1994b) and WAGNER et al. (1994). Based on the methods of HIRSCHWALD (1911) and BENTZ & MARTINI (1968), the quantity of mica layers/mm and the thickness of the mica layers can be measured and their structural network can be estimated. The quantile can be determined from the quantity of the mica layers and their thickness.

Quantile = 10 times the thickness multiplied by the number of mica layers.

The quantile indicates the percentage by volume of the minerals, which form the cleavage surfaces and thus the cleavability. The number of mica layers and the quantile of the investigated samples are considerably above the minimum values for roofing slates, namely, 40 mica layers/mm and a quantile of 0.4 (cf. table 4).

The scanning electron microscope investigations document both the orientation and the new growth of mica. Particularly interesting in this context is a comparison between two occurrences, that of Penrhyn and the Escorial slates (Bernados, Prov. Segovia/Central Spain). It can be observed here what WEBER described (1976). In the case of the Penrhyn slate (cf. Chapter 1.4), the mica orientation is poor, partially appearing as a flexure in the cleavage surfaces. In contrast, the Escorial slate with its noticeably higher level of metamorphosed phyllites (Bernados, cf. fig. 3, no. 9), allows a clear orientation due to new growth of mica. As far as the phyllite in sample VII is concerned, the higher level of metamorphosis can also be recognized by the higher quantile using a light microscope (cf. table 1). All other slates range between the extremes described above. What strikes is that almost all slates can be characterized by new formations of phyllosilicate parallel to the cleavage, as described by WEBER (1976). In the slates of the East Eifel area, flexures are also present. The higher metamorphic grade of the Spanish slates can be recognized by the somewhat better orientated phyllo-silicates.

Due to the small grain size of the minerals in slates, the modal mineral composition can be determined with great difficulties, only. Therefore, table 1, only shows the determination of porphyroblasts and the estimate of the mineral content of the groundmass. Only with the assistance of chemical analysis (table 3) and microscopic analyses, is it possible to make an estimate as to the modal mineral composition (cf. table 2). As expected, all investigated slate samples consist primarily of sericite. Large muscovites and paragonite (Na mica), which can only clearly be detected by x-ray analysis, are also to be found. The sericite content (including muscovite and paragonite) varies between 40 and 50 %. This value was fallen short of only once when slates with a high carbonate content (sample V) were investigated.

More obvious differences are present when considering the chlorite content. Amongst the slates with a low carbonate content, the chlorite content was somewhat lower in sample I as compared with II and III, and in sample VI (Spanish) the chlorite content was among the highest (27 - 28 %). On the whole, the chlorite content varies between 20 and 28 % and, again, is only significantly lower in slates with a high carbonate content (samples IV and V). Sample VII is a phyllitic chlorite slate where ferric chlorites predominates.

The quartz content varies between 23 and 35 %. In samples I, III, V and VI, 5 different tiles were examined. Even in the tiles of just one sample, the quartz content differs considerably, which may be explained by varying sedimentary sand intercalation in the individual slate tiles.

The various minerals have an influence on the technical behaviour and the durability of the slate. A survey on this subject was provided by BENTZ & MARTINI (1968). According to their theory, the sericite content ought to be around 40 % and this is important for the cleavage and thus the cleavability.

The quartz content is important for the strength of the slate. A high content can have negative effects on the processing of the slate and the ability to punch holes in the material. It only has a negative influence on the cleavability if the orientation of the quartz along the cleavage is incomplete.

As a result of an investigation of old roofings in the Netherlands, VAN RHIJN & MELKERT (1993) developed a classification system for slate qualities, which is organised into a complicated tree structure based on petrographic observations and can estimate the durability of the slates based on the modal mineral composition.

Good = durability of more than 80 years
Medium = durability of 50 to 80 years
Bad = durability of less than 50 years

The way in which these characteristics relate to the mineral composition, is displayed in a simplified form in table 2, where the evaluation is simply indicated as positive or negative. The classification into good, medium and bad is not very helpful in the evaluation of occurrences as shown by the test series since even relatively consistent occurrences vary within certain limits and thus may often be classified in different categories simultaneously.

Taking VAN RHIJN & MELKERT'S judgement as a basis, samples I and III could be classified as good and samples II and III as bad. Although their work includes many interesting details and observations, reliability in respect to contemporary slate occurrence is limited. Their study is focusing purely on older roofings, that means, on a small selection of slate types, which are still available on the market today. As fa as the samples of the test series are concerned, only the quarries of samples I, IV and V have been in operation for more than fifty years. All other extraction areas have been in use for twenty to thirty years, only (also II and III). From the investigation of the characteristics and the evaluation of the observations of this selection of slates, VAN RHIJN & MELKERT define various demands without proving precisely that the characteristic or the observation is the cause for the susceptibility to degradation. Thus, the ratio of chlorite/sericite (including muscovites etc.) is used for a quality judgement without clarifying whether this is a true cause for resistance to disintegration or lack of resistance. It is also possible that a higher ratio was merely a random characteristic of the slates, which did not have such a durability on old roofs for completely different reasons. Nevertheless, the work shows conclusions on carbonate content and structural investigations, which were confirmed by our own research.

Mineral content, microstructure, and the other petrographic characteristics of slate play an important part as far as the quality and the processing of slates are concerned. It is worth noting, however, that the relationships of these different characteristics are extremely complicated and, in general, it is not possible to evaluate the slate by just one single characteristic. The weathering of various minerals (for example, carbonate, some types of ore) can be reduced if these are incorporated inside the protective mica structure.

3. Chemical analyses of argillaceous slates

The petrographical/mineralogical analysis is reflected in some respects in the chemical analysis, although a chemical analysis states less on the technical properties than a thin section analysis. Series analyses were made on the main elements and on CaO and/or MgO (tables 3 to 9) dissoluble in acetic acid and also on some trace elements from specifically chosen samples (tables 4, 6, 7). In the series analyses, the CO_2 content, the water (H_2O+, H_2O-) as well as the SO_2 and SO_3 content are contained within the loss of ignition.

A comparison of the analyses of the various occurrences reveals that it is not possible to clearly identify the individual occurrences with the aid of these analyses, although it is possible to differentiate between some regions. The analyses of samples IV and V clearly indicate, by their high CaO content and loss of ignition, the consequences of high carbonate content. Slate sample IV has 52 - 53 mass-% of SiO_2 and 5.5 to 6.66 mass-% of CaO. The ratio of Na_2O to K_2O is around 1:3 to 1:4. In contrast, the CaO content in sample V is higher (8.5-11 mass-%) and the Al_2O_3 content is around 1 % less. The loss of ignition is considerably higher due to the high carbonate content.

The TiO_2 content of sample IV lies at 0.76 % whilst this value lies at 0.68 % in the extraction area (sample V) adjacent to the former. These carbonate-rich Sauerland slates can be clearly distinguished from those of Rhineland-Palatinate, i.e. the almost carbonate-free

slates of the Hunsrück (samples II and III) and the East Eifel slates (sample I amongst others).

The slates of the Hunsrück area show a higher Al_2O_3 content (18-21 mass-%) when compared with the Sauerland slates; their CaO content varies between 0.5 and 0.9 mass-%. The Na_2O:K_2O ratio lies at around 1:3 to 1:4. The slates of the East Eifel (Mosel slates, amongst others, sample I) are very similar; their CaO content varies between 0.39 and 1.41 mass-%. On the average, the Mg-O content is lower than that of the Sauerland slates. Whilst the slates of the East Eifel have a mean SiO_2 content of between 56 and 58 mass-%, that of the Thuringian slates (cf. table 5, no. 2) is surprisingly high (appr. 62 mass-%). Their CaO content is low, as is the loss of ignition.

The important group of the Spanish slates of the Valdeorras region (Galicia) are, with one exception, distinguishing by their low CaO content (cf. table 6), which is also reflected in the low loss of ignition. Noticeable is the generally higher Al_2O_3 content in comparison with sample I, as well as the considerably higher Na_2O/K_2O ratio, which is often greater than 1:5. Another characteristic is the MgO content which is often less than 2 % (around 1.75 %).

In view of the incomplete data, it is at this point unnecessary to discuss the full analyses of the other occurrences (cf. tables 7 to 9). Worth mentioning, however, is the occurrence of Penryhn, North Wales, where the SiO_2 content lies at around 59 mass-% and the Al_2O_3 content of which is around 20 mass-%. These slates are particularly extraordinary due to the fact that the Fe_2O_3 content is around 8% (red, haematite-rich slates) whereas, in the German and Spanish slates, this value is usually around 1 %, with the exception of Thuringian slates, where the Fe_2O_3 value varies between 0.08 and 0.48 %. Penryhn is also noteworthy because of its Na_2O/K_2O ratio of around 1:1.5.

In view of the variation of the trace element contents (tables 4 and 6) we only made a comparison of analyses between the slates of the East Eifel and the Spanish slates of the Valdeorras. The interpretation allowed us to make the following careful conclusions:

- The lead (Pb) content is generally around four to five times higher in the Spanish slates as compared with slates from the East Eifel. The maximum value recorded was around 20 ppm.
- The nickel (Ni) concentrations are enriched by 150 to 200 % in the East Eifel slates (approx. 75 ppm to 35 ppm).
- The chromium (Cr) content is higher in the East Eifel slates than in the Spanish slates.

In summary, it can be stated that except for the CaO content and the other minor discrepancies listed above, the chemical composition is more or less identical for all roofing slates, even or slates from overseas (cf. table 9), regardless of their quality and geology. Chemical analysis thus presents very little quality-relevant information. When considering non-quality related parameters, small differences between the various occurrences turn up, which could possibly be used as distinguishing characteristics and as a basis for further research. Therefore, the complete chemical analyses are displayed in tables 3 to 9.

4. Petrophysical investigations on roofing slates

4.1 Preliminary remarks

A number of test standards have been in force for some decades regarding the petrophysical characterization of roofing slates. These standards, however, are generally ignored since they only allow the exclusion of entirely unsuitable roofing slates, an expert being able to do this without time consuming and expensive investigations. The reasons for the poor efficiency of previous petrophysical investigations include, to some extent, unsuitable sampling methods, but also, obsolete measurement techniques and unreproducible test series. Our petrophysical investigations were applied with regard to these two points.

The test standards so far applied to roofing slates are:

DIN 52 101 (sampling)
DIN 52 102 (bulk density, true density, density grade, true porosity)
DIN 52 103 (water absorption and saturation coefficient)
DIN 52 104 (freeze-thaw cycle test)
DIN 52 112 (bending test)
DIN 52 204 (thermal cycle test)
DIN 52 206 (acid test)

As far as the results of the bending test acc. to DIN 52 112 were concerned, we did not take the calculated peak strength as a basis, but a peak load per 1 mm thickness of the slate. This was done for better comparability. One problem in all petrophysical investigations is the fact that random samples were used which might not be representative for a larger occurence.

The concept of roofing slates and the evaluation of the above testing methods are defined in DIN 52 201. The method of sampling is regulated by DIN 52 101. The testing methods described in the above-mentioned standards are certainly suited to determine petrophysical parameters from a physical point of view. Thus, it was attempted to establish the causes for the wide variety of values measured in the individual investigations and for the fact that the test results were not reproducible .

Since the testing methods for roofing slates, as applied at present, primarily produce qualitative statements which are often unquantifiable, the first thought was which physical property of the rock changes quantifiably during as many testing methods as possible, whilst a reproducibility of these measurements should be possible as well. Both the freeze-thaw test and the thermal cycle test result in structural disintegration when problematic rocks are tested and in some extreme cases, for example, by the acid test, the sample can be destroyed. Such changes in physical condition can be measured by a compression wave velocity test, for instance. Ultrasound waves are particularly suited for this purpose due to their short wave-length. They are often used in material testing (fig. 6).

4.2 Ultrasound wave velocities for the quantification of structural disintegration

For material testing, ultrasound waves are used primarily in view of their wave velocity and signal damping. As far as the slates to be investigated are concerned, the signal damping is difficult to measure (probe coupling). Therefore, the signal damping was not measured, only the wave velocity and its change during petrophysical investigation. The compression wave velocity in roofing slates can provide evidence for the water absorption and the bending strength of a slate tile.

A preliminary selection of transducer probes was made following references in literature, in particular, KRAUTKRÄMER & KRAUTKRÄMER (1986). Twin transducer probes proved to be unsuitable after the first tests and thus the investigations were carried out using a separate transmitter and receiver. In general, a high frequency of the probes is preferable, but it must be noted that with an increase in frequency, the power of the transmitter must also be increased. After a few initial attempts, highly dampened 1 MHz - 2 MHz probes were settled upon.

The probe coupling was achieved using a direct contact and coupling paste. Due to surface roughness of the slate tile, the coupling was often unsatisfactory and thus a system with water probes had to be created.

After further investigations of roofing slate tiles, such as, for example, samples I and VII (cf. with Chapter 1), it became evident that the wave velocity was heavily influenced by the water saturation of the slate (fig. 7). Thus, in subsequent investigations, the wave velocities were measured in water saturated slates.

For the determination of the wave velocities, the thickness of the test specimen was measured as accurately as possible, since the calculated wave velocity at a given transit time is directly proportional to the test specimen thickness. This problem of thickness measurement can lead to severe problems in roofing slates, since the surfaces are irregular and not always with parallel faces. The relatively imprecise thickness measurement is thus a decisive factor for the measurement accuracy. The smoothing of the surfaces is no solution either, since the physical properties of the tile may be changed in an uncontrolled way. The precision of a single wave velocity measurement is around 100 m/s and in exceptional cases 200 m/s.

After a review of various test records on the technical investigations acc. to current DIN standards such as thermal cycle tests (TW), freeze-thaw tests (FTW) and acid tests (SV) on roofing slates, it became evident that the usual recording of mass losses of the slate tiles during these investigations could not provide satisfactory quantitative statements on the reduction in quality due to the investigative methods. Due to the reasons described above, we expanded the thermal cycle tests, freeze-thaw tests and the acid tests in such a way that the ultrasound wave velocity of the tiles was recorded both before and after the relevant test. The measuring direction was always normal to the cleavage. After initially successful results, problems arose with the reproducibility of the wave velocities. We concluded that the wave velocities are strongly dependent on the degree of water saturation of the tiles. The DIN standards for the thermal cycle tests and the freeze-thaw tests recommend the use of air dry specimens. However, how does one define air dry? When does a tile which was been dried to 110°C have the water content of an "air dry" tile? Thus, wave velocities should only be measured on tiles previously saturated with

water. Following this precondition, the velocities are reproducible. A further improvement in the measurements was achieved by the water coupling, as described above.

4.3 Anisotropy of the ultrasound wave velocity within the cleavage planes

The level of metamorphosis of a slate (i.e. the extent of the influence of temperature and pressure on the slate since its formation) can vary quite considerably and could have an influence on the petrophysical characteristics. The anisotropic deformations which such a rock undergoes on the cleavage plane can be traced by examining, for example, fossils embedded therein. In the same way, this deformation affects the orientation of minerals. Since minerals, with respect to their physical characteristics, are generally anisotropic, the level of the mineral orientation of the slates can be determined with the help of ultrasound wave velocities.

In order to determine the anisotropy of the propagation of the ultrasound waves in the cleavage plane, regular dodecagons were created and submitted to ultrasound analysis. With this investigative technique, the velocity of the ultrasound waves could be measured in six different directions. This proved to be sufficient for the purposes of this investigation. The results, as recorded in the measurements of the slate tiles, showed that better data were obtained where water coupling was applied.

The anisotropy of the ultrasound wave velocities in the cleavage plane was recorded for forty-five European roofing slates. The measurements were recorded in a graph, with the directional azimuth of the measurements as the X axis and the wave velocities as the Y axis. A cubic spline was calculated from the values and portrayed as a curve. This cubic spline shows a simple progression between two extreme values in virtually all samples over the 360 degrees of the measurement azimuth (a velocity minimum and a velocity maximum; cf. fig. 8, 9, and 10). Splines with a higher frequency are exceptional and can be seen in three of twenty-one samples from Spain and the samples from occurrence V (cf. fig. 11 and 12). In these samples, the additional minima and maxima can be explained by the presence of micro-cracks. Mostly two maxima and minima are shown, with the maximum, as a rule, running normal to the cleavage and the minimum running vertically to it, if stratification is not macroscopically detectable. If stratification is macroscopically detectable, then the velocity of the ultrasound waves is at its greatest parallel to the direction of the delta axis of the stratification and at its smallest at right angles to this plane. This direction is known in Spain as the so-called ”longrain”. In slates with ”longrain”, this plane is that of the lowest durability (cf. DIN prEN 12 326).

No quality criteria could be gained from the experiments conducted using the velocity anisotropy of ultrasound waves in the cleavage plane.

4.4 Results of the petrophysical investigations in a test series on samples from seven selected regions.

As described in chapter 1, samples were taken from locations I, II, III, IV, V, VI, and VII. The sampling of the roofing slates was done as prescribed in DIN 52 101.

Samples I to V were taken in the presence of a geologist and/or at least one company representative. The splitting and processing of the tiles was undertaken in the presence of above-mentioned persons on the same day by the employees of the respective firm. Before splitting, blocks of 100 mm width and 200 mm length were cut with diamond-bladed saws.

The slates, samples VI and VII were taken from one deposit and processed at the University of Trier into tiles of 100 mm by 200 mm size using diamond-bladed saws. The quality of these Spanish roofing slates cannot be considered as typical for Spanish slates. Sample VI was chosen because it came from a new open-cast mine and also because it came from the surface, thus from an area which does not yet display the quality of a sample taken after extensive mining. For comparative petrophysical studies, a slate of questionable quality may serve as a point of reference.

Sample VII was incorporated into the investigations as a phyllitic slate due to its higher level of metamorphosis in comparison to the slates mentioned above.

The raw density and water absorption of the seven different roofing slate varieties was recorded and an acid test, a thermal cycle test, a freeze-thaw test, a bending test, and ultrasound measurements were carried out both alone and in combination with each other. For a better view, a flow diagram was developed (cf. fig. 6), which shows the type, quantity and combination of the various petrophysical investigations implemented on the samples. In some experiments, the number of freeze-thaw cycles, for instance, was changed as against the DIN standard (cf. Table 10) in order to study the influence of differing cycle numbers. These changes are indicated in the diagram.

The results of the petrophysical investigations on the various sample areas are portrayed separately and peculiarities are indicated. In the final part of this section the measurement data are considered and interpreted as a whole.

Sample I

The petrophysical investigations and testing methods were started with tiles from sample I. Due to their general importance, two results of these investigations are portrayed here in the form of diagrams.

The velocity of compression waves, running normal to the cleavage was measured for approx. 240 roofing slate tiles (fig. 8). The specimens were air dry and were measured in direct contact with coupling paste. The average value of 4617 m/s was represented in the great majority of recorded measurements. There were however a noticeable quantity of samples which displayed values that were considerably higher or lower. This shows that the velocity alone is only of limited use in making a quality assessment. Of considerably more importance are the differences in velocity, which were recorded before and after a petrophysical experiment on the same tiles. Nevertheless, a rough quality assessment can be deduced from the mean velocity value. The investigations showed that roofing slates where the velocity lies below 3000 m/s are generally of a lower quality (see table 12, in air dry condition, normal to the cleavage).

With slates which underwent the freeze-thaw test, with 50 cycles, the water absorption was recorded before the experiment, after 25 cycles and at the end of the experiment.

To our surprise, the respective water absorption values showed only a minimal increase after 50 freeze-thaw cycles, specifically from 0.32 % by weight to 0.37 % by weight. The water absorption after 25 cycles had not changed in any way when compared to the pre-investigation status. The reduction in quality thus does not follow in a linear manner the demands placed on the samples. For a representative petrophysical investigation, it would be advantageous to implement as many cycles as possible on a larger quantity of specimens.

It is worth noting that, in the freeze-thaw test with 25 cycles the water absorption under atmospheric pressure increases (cf. table 10), whilst the water absorption in the autoclaves at 150 bar pressure returns to a value identical to the value before the beginning of the test. This shows a special pore structure. In a normal water absorption test, made under pressure, the water is able to spread sufficiently through all the pores. The pressure effect in the freeze blasting as in the freeze-thaw test does not exceed these pressure relationships and thus does not lead to a higher water absorption.

The bending tests on water saturated, unimpaired tiles and on tiles which underwent an acid test, a thermal cycle test, and a freeze-thaw test showed a bending strength per 1 mm tile thickness of 76 Newton (N), 71 N, 66 N, and 74 N. It was obvious that there was only a minor quality reduction of the roofing slates as a result of these tests. The bending tests, however, also showed that it is important to maintain comparative conditions when carrying out these tests. This does not just mean an equal rate of load application, but also an equal water content in the specimens. This becomes evident by the two freeze-thaw tests with subsequent bending test. If the normalized bending strength without previous tests was 101 N for air dry tiles and 76 N for water saturated tiles, then the normalized bending strength after the freeze-thaw test was 108 N for air dry tiles and 74 N for water-saturated samples. From these data, we can infer that the expression air dry, as a description for the water content as used in the DIN standards, should be rejected, since an air dry condition cannot be reproduced. The reason for this is that the normalized bending strength after the freeze-thaw test (108 N) lies between the value for the dry (110 °), untreated samples (110 N) and the air dry, untreated samples (101 N) (cf. table 11).

The change in the ultrasound wave velocities, as carried out in the petrophysical investigations, produces a similar picture to that of the bending test. The wave velocity is only reduced by a few 100 m/s. Naturally, a precondition for this test is also an equal, defined water content (cf. table 12).

Sample II

The roofing slates used for these petrophysical tests have average values when compared with the test results of the other locations. Of particular interest is the noticeable change in the physical characteristic values during the acid test (see tables 11 and 12). In this case, there is a significant difference between this sample and the results obtained for samples I, III, VI, and VII.

Sample III

In all tests, the samples of this roofing slate showed petrophysical characteristic values which were above average (in comparison with the samples taken from other locations). In particular, hardly any material changes were noticed after the freeze-thaw

test in both the ultrasound wave velocities running normal to the cleavage (4128 m/s before the freeze-thaw test and 4114 m/s after the test) and the normalized bending strength (111 N before the freeze-thaw test and 95 N after freeze-thaw test I and 100 N after freeze-thaw test II) (cf. table 11).

Sample IV

Like sample V, this sample is characterized by a higher carbonate content. This was explicitly evident in the results of the acid test. The normalized bending strength was reduced to around 1/3 (air dry and water saturated) of the initial strength (cf. table 11, fig. 13). The ultrasound wave velocity normal to the cleavage changed considerably. From the ten tiles used in the acid test (five air dry tiles and five water-saturated tiles), it was only possible to carry out an ultrasound wave velocity test on one of the tiles. The disintegration in the cleavage was so strong in all the other tiles that the transmission strength of the ultrasound device was too low to penetrate the tiles.

The water absorption of the tiles, at 0.68 % by weight (cf. table 10) (without previous tests) lies above the critical value (0.5 %) prescribed for weathering in the European standard, DIN 52 106. The European standard, DIN prEN 12 326, Part 1, prescribes a value of 0.6 % (slates with higher values must undergo one hundred cycles of freeze-thaw tests).

The behaviour of the tiles in the thermal cycle tests and in the freeze-thaw tests was, however, faultless. The bending tests carried out after two freeze-thaw tests prove that if the bending test is carried out properly (water content!) then the changes in the material properties can be reproduced. If the normalized bending strength of the tiles without previous treatment was 78 N, then the value was at 72 N, on the average, and/or 71 N after the freeze-thaw test. The ultrasound wave velocities normal to the cleavage showed no material changes within the scope of the accuracy of measurement.

Sample V

As in sample IV, this slate displays severe disintegration after the acid test. In particular, the tiles which were subjected to the Acid test in an air dry state showed a significantly lower level of disintegration. The ultrasound wave velocity normal to the cleavage was still measurable after the acid test in all five specimens (before the acid test: 4118 m/s, after the acid test: 2552 m/s; cf. table 12). Despite a higher carbonate content than that of the slates from sample IV, the specimens showed a greater durability in the acid test. The reason for the lesser degree of damage may be due to the higher raw density, but also and more likely due to the lower level of water absorption (0.54 % by weight). The tiles showed average values in the thermal cycle test and in the freeze-thaw test (see table 11).

Sample VI

With the exception of the results from the acid test, the petrophysical investigations (freeze-thaw test, thermal cycle test and bending test) which were carried out on samples VI showed the worst characteristics of all the test subjects (cf. tables 10 and 11). This is particularly obvious in the water absorption value of more than 1 % by weight). This water absorption rate is more than twice the amount prescribed by the DIN 52 106 standard

(basic estimation value for weather durability) for slates of restricted use or non-weather proof slates.

Sample VII

All roofing slates from location VII showed an average level in all petrophysical investigations. The wide spread of petrophysical values within individual specimens is particularly striking as far as these samples are concerned. For example, the normalized bending strength for water saturated tiles, without previous tests was 49 N; and after the acid test (water-saturated), this value was at 75 N. The water absorption after 25 freeze-thaw cycles rose from 0.38 % by weight to 0.45 % by weight and thus indicates a strong change in the petrophysical parameters as a result of the freeze-thaw test (see table 10).

4.5 Summarized observations with regard to the individual petrophysical methods

In Chapter 4.4, the results of the various petrophyscial investigations on the samples from the seven roofing slate locations were portrayed. Peculiarities in the individual investigations were pursued. The petrographic parameters yielded by these investigations will be interpreted in the following section and their suitability for a petrophysicallly-based quality assessment of roofing slates will be evaluated.

- Water absorption and raw density

The water absorption of roofing slates before and after the petrophysical investigations is portrayed in table 10, i.e. the mean value of five tiles. The mean values for raw density are also shown in the same table. A clear connection can be ascertained between these two values. A low raw density correlates with a high level of water absorption and a high raw density with lower water absorption (cf. fig. 14). The roofing slate samples I and II show the highest raw densities (2.78 g/cm3, 2.79 g/cm3) and the lowest level of water absorption (0.32 and 0.38 % by weight). The lowest raw density (2.72 g/cm3) and the highest water absorption (1.11 % weight) can be found in the tiles from sample VI. The other locations show values which lie between these extreme values. The parameters raw density and water absorption alone appear to reflect a quality estimation that can be confirmed by other petrophysical investigations. Namely, a high raw density and low water absorption level can be found in a slate with good petrophysical values and low raw density and high water absorption for a slate with poor petrophysical values.

A similar picture is displayed in the ultrasound wave velocity investigations of the above tiles. Samples I and III show high wave velocities (4912 m/s and 4727 m/s) whereas VI shows a low wave velocity (3631 m/s, cf. Table 12).

In addition to the water absorption under atmospheric pressure (Wm, a), the water absorption under pressure (Wm, d) was also recorded in an autoclave at 150 bar hydrostatic pressure. This parameter did not, however, yield any new information since the water absorption values under atmospheric temperature and at 150 bar were exactly the same within the scope of the measurement accuracy (cf. table 10).

According to the German natural rock standard (DIN 52 106), importance is particularly attributed to water absorption under pressure, when the water absorption under

pressure is significantly higher than that under atmospheric pressure. This is expressed as the saturation value (quotient Wm, a to Wm, d) which is seen as positive when the value is below 0.75. The roofing slates investigated in this experiment, however, possess generally higher levels of saturation (as is expected in the majority of good quality roofing slates), see Table 10).

- Bending test

There are three factors of decisive importance for the reproducibility of the bending tests. If the bending test is carried out on air dry tiles, this often leads to results that cannot be reproduced for the previously noted reasons. Investigations were carried out on dried (at 110°C), air dry and water-saturated tiles for all localities (see Table 11). The standardized bending strength can be changed by up to 100 % purely by varying the levels of water content in the investigated tiles. Following DIN 52 112, the results of this experiment are portrayed through the breaking load applicable to the roofing slates. This, however, leads to results that cannot be reproduced since the thickness of the slates (with an average of 6 mm) can vary from 5 - 7 mm. As a result of these variations in tile thickness, the breaking load can also change by a third (precondition: breaking load is proportional to tile thickness). A noticeable improvement in the reproducibility of the data was observed when the breaking load was normalized to 1 m thickness. This normalized value was then used for all bending tests. The conversion of the breaking load into a value for bending strength, as per DIN 52 112, leads to atypical values in roofing slates. This formula, which was developed for other types of natural rock, is limited by the clear anisotropy displayed by roofing slate and is thus not transferable. It is important that all tests are carried out with the same load increase. If these points are considered, then the standardized bending strength can be reproduced. Two series of the bending tests on water satured tiles from three locations (samples III, VI, and V) after 25 freeze-thaw tests, each, prove this (an average value each from 10 tests):

Locality	standardized bending strenght (N)	
	Test I	Test II
III	95	100
IV	72	71
V	65	69

In these examples, the variation between bending test I and bending test II is less than 5 %. The influence of air dry and/or water-saturated tiles on the standardized bending strength is shown by two bending test results on the tiles from sample I. Although the air dry tiles were subjected to 50 freeze-thaw tests and the water-saturated ones to only 25 freeze-thaw tests, the standardized bending strength of the air dry tiles was 108 N and that of the water-saturated tiles only 74N.

From the test results we can ascertain that the bending test can be used to characterize the petrophysical changes of roofing slate tiles in the acid test, the thermal cycle test and the freeze-thaw test, if the conditions noted above are observed. Differences in quality can easily be observed. In the Austrian natural rock standard system, a remaining durability of less than 80 % after 25 freeze-thaw tests is seen as problematic (Önorm B 3123-1 1990) (cf. Table 11).

- Acid test

The acid tests were carried out in accordance to DIN 52 206. Afterwards, the tiles were also subjected to a bending test. The ultrasound wave velocity normal to the cleavage was measured both before and after the start of the investigation. The DIN 52 206 standard evaluates the effect of the acid test through the change in mass in the roofing slate tiles which are placed in the acid. The mass change, the change in the ultrasound wave velocity and in the standardized bending strength were all utilised in the characterisation of the roofing slate changes. In addition, the macroscopically observed changes in the tiles, such as colour, coating and fissure formation were also noted. All four recorded and observed parameters clearly show two groups of roofing slates after the acid test. Samples I, III, VI and VII showed only minor changes in response to the acid test, whereas samples IV and V changed dramatically in their physical values dramatically (cf. Tables 11 and 12). Sample II can be placed roughly in the middle of these two groups. Not all of the four parameters are, however, equally suited to characterize the changes in the roofing slates. The mass changes appear to be the critical value. Sample III shows an average mass change of 0.32 % for the water-saturated tiles and 0.39 % for the air dry tiles. Bending strength (102N and 102N) and ultrasound wave velocity changes (-347m/s and -390 m/s) display virtually identical values for both water-saturated and air-dried tiles (cf. fig. 13). The air dry samples VI and VII show a mass deficit (splintering) after fourteen days. After twenty-eight days, they showed an increase in mass like all other samples. The changes induced by the acid test can be most clearly seen in the ultrasound wave velocities. The water-saturated samples IV and V had changed so dramatically that it was no longer possible to take measurements. In the air dry tiles, it can be seen that sample V was less damaged than sample IV (with sample IV, the ultrasound wave velocity could only be measured on one tile and with sample V, it was possible on all five tiles).

In the interpretation of the bending strength values made after the acid test, it becomes evident from the results that the standardized bending strength drops less in thick tiles than in thin tiles (this can be explained by the fact that the tiles were subjected to acid corrosion from the surface). The influential factor, tile thickness, is thus not arithmetically correctable. This is a considerable difference compared with the other bending tests carried out. Thus, for the acid test, tiles of equal thickness should always be used. This can be proven by an example taken from tiles of sample VI. The mean value of the standardized bending strength is 60 N for air dry tiles and 114 N for water-saturated tiles, although the water-saturated tiles usually change to a much greater degree during the acid test and thus their breaking load, in comparison to the air dry tiles is lower. The water-saturated tiles, however, have a thickness of up to 7.45 mm, whereas the air dry tiles only up to 5.5 mm. A comparison of the standardized bending strength from air dry tiles of varying thicknesses also demonstrates the same effect after the acid test. The thickest tile, with a thickness of 5.5 mm has a standardized bending strength of 85 N and the thinnest tile, with a thickness of 4.0 mm has a standardized bending strength of 30 N.

In the macroscopic investigation of the tiles after the acid test, small tight balls were visible after drying out, particularly in samples I and VI. These balls became dull after a certain time and then took on a light yellowish-green hue. When seen X-rayed, it is clear that this phenomenon is due to a melanterite ($FeSO_4 \times 7H_2O$). This mineral occurs as a new formation, for example from sulphuric pyrite and can be washed away.

-Long-term acid test

In most tests made on materials, and thus also on natural rock and on roofing slates, we are dealing with so-called “time-lapse” tests. The first objective of such a test is the reproducibility. However, the question of how such a test, with its inherent long-term environmental conditions, can be successfully represented is often considered less important (cf. WAGNER 1996). In the compilation of the prEN 12 326 standard, the acid test was the primary subject of discussion. In addition, the question arose as to what degree the long-term effects, in cases of good slate quality, without carbonate content, can be predicted in a test with a time limit of only twenty-eight days (as specified in the DIN 52 206 standard). It is well known that roofing slates of good quality last extraordinarily long (often longer than the accessories, for example, nails or the support beams). However, atmospheric conditions in the last few decades have become noticeably worse (Keyword: acid rain, which the acid test is supposed to portray), and there are weather-related disintegration processes now which did not exist before. As a result, poor quality slates will disintegrate faster. But what about high quality slates? Will they also last for 200 years given the present atmospheric conditions?

These considerations and the results explained above led to a five year long-term test undertaken by the company Rathscheck. The test conditions follow the DIN 52 206 standard, although the weight checks were carried out at greater intervals.

The test was initially carried out on slates with carbonate content (for example, sample IV amongst others). A colour change occurred after only a few days, from the original colour of blue-black to a light grey. After some weeks, the slates slowly began to disintegrate. The first occurrence of structural disintegration happened in the first few weeks. Disintegration progressed from this point so that after 200 to 300 days the tiles under investigation were totally destroyed and could only be preserved in the test environment with the aid of supportive measures (plastic foil with holes).

These processes, including the colour change, appear at first to be connected to the alteration of carbonate to gypsum. During this process the mass increases considerably. After the first occurrence of structural damage, approx. 200 to 300 days after the start of the test, the velocity of mass increase slows down (see fig. 15). However, after five years there is still a clear mass increase, even with an advanced state of structural disintegration. The investigated slates thus, did not form a protective layer of gypsum as is the case with some other carbonate based rocks.

A stochiometric examination of the metamorphic process of calcium carbonate ($CaCO_3$) into gypsum ($CaSO_4$ x 2 H_2O) shows that this process can in no way explain the total change in mass, but rather only the most noticeable change in the first 200 to 300 days up until the clear disintegration of the structure. A mass change of only around 7 – 15 % is to be expected from the formation of gypsum (in cases of calcium carbonate content of 10 to 20 %). The mass increases after this point can be traced back to other processes, partially also due to the significant level of water absorption present in the heavily disintegrated sample. Two control readings, made after 2200 days, showed a mass loss up to a constant level of weight of 12.4 % to 17.4 %, after drying out at 40°C (after four days) and after drying out at 110°C, an additional mass reduction of 10.7 % (and/or 8.7 %).

If a carbonate-free slate is observed (for example, sample I), then it can be seen that the behaviour of the slate after the first 24 days (normal test period of DIN 52 206) can be applied to much longer time periods, for example five years. With the exception of the previously mentioned colour changes, there were no other changes in the slates even after such a long period of time. The mass increase was 0.6 % at maximum. In comparison to this, weight increases of 51 % (sample IV) or even up to 70 % were observed in other carbonate rich slates (cf. fig. 15).

In addition, a long-term acid test with asbestos cement also proves informative. The structural durability of the asbestos-cement mixture remained stable even over a very large time-span. It is, however, critical to assess the fact that fibres began to separate themselves from the tiles after only 400 days. The often uttered request to leave the numerous asbestos-cement roofs untouched and to refrain from an expensive removal with the accompanying asbestos-related risks is not supported by these results.

Despite these very interesting results, long term tests naturally do not enhance the debate on standards significantly, since the examination of materials does demand, quite correctly, manageable and thus practical test periods. On the other hand, research conditions should not be reduced to such an extent (as suggested in HEISS & ZALLMANZIG 1994 and KIRCHENER & ZALLMANZIG 1995 on grounds of fewer test results from the regionally limited areas of samples IV and V) that no reactions characteristic for some type of slates occur at all during the test period. Furthermore, it has to be taken into account that with a limited acid supply in the test period, slates with a high carbonate content may display untypically positive values, since the acid may be buffered early on due to the carbonate content of the samples.

- Thermal cycle test (TW)

The effect of the thermal cycle test was described according to DIN 52 204, and emphasis was placed on macroscopic observation of the changes in the slates during the test.

In addition, the bending test can be incorporated after the experiment for additional comment. In this project, the ultrasound wave velocities of the roofing slates both before and after the tests were also measured and the mass loss as a result of the test was determined. The tiles of samples I, VI and VII were subjected to 35 temperature cycles and those of samples II, III, IV and V were subjected only to 25 (following the DIN 52 204 recommendation). A compilation of the data is presented in Tables 11 and 12.

During the tests, it became apparent that the varying number of temperature cycles had little influence on the normalized bending strength recorded after the tests or on the changes in the ultrasound wave velocity. In general, the reduction of the normalized bending strength is no larger than 25%, with the best value being at < 2 % (sample IV). The reproductibility of the normalized bending strength ranges from good to acceptable (in each case, the average was taken from ten values).

Locality	Normalized Bending Strength (N)	
	Test I	Test II
III	74	94
IV	77	70
V	58	60

The ultrasound wave velocity shows that during the test there was no significant decrease. This does not apply to sample VI, which displayed the greatest velocity differences (reduction of 12.1 %) and sample VII, which displayed a very low ultrasound wave velocity both before and after the test (2958/2780 m/s). Samples VI and VII displayed the lowest normalized bending strength after the thermal cycle test (48 N/37 N). The mass deficit was also at its greatest in these two slates at 0.06 % and 0.08 %.

-Freeze-thaw test (FTW)

The effects of the freeze-thaw test (FTW) were recorded, in accordance with the DIN 52 104 standard, through observation of the loss in weight during the test and, where necessary, through an additional bending test. Furthermore, in this project, ultrasound investigations were carried out on all samples, both before and after the tests. Additional measurements of water absorption under atmospheric pressure and under 150 bar were also taken for specimens from samples I, VI, and VII. A compilation of the data is presented in Table 10.

Samples VI and VII deviated in their mass deficit quite considerably from the other samples, with values of 0.08 % and 0.2 %. Samples I to V showed a certain degree of consistency with values ranging from 0.05% to 0.06%. It can be observed that the tiles from sample I, in an air dry state and after 50 freeze-thaw tests were significantly better in the normalized bending strength than those of samples VI and VII (I = 108 N; VII =72 N/80 N; VI = 84 N/98 N). After 25 freeze-thaw tests (made on water-saturated tiles), samples I, II, IV, and V lay at around the same level in the normalized bending strength. The tiles from the locality III lie considerably higher with a normalized bending strength of 95 N/100 N which may, however, be traced back to the generally higher normalized bending strength of the untreated tiles. The percentage reduction is similar to slates I, II, IV, and V.

The ultrasound wave velocity measurements with the process of water coupling (samples II, III, IV, and V) display similar results to the normalized bending strength values (cf. Table 12). The tiles from samples II, III, IV, and V display virtually no loss in ultrasound wave velocity and are thus hardly damaged at all by the freeze-thaw tests. The ultrasound wave velocity measurements made on samples I, VI, and VII are, however, not directly comparable, since they were examined with a different investigative method and without observation of the precise water content.

Ultrasound wave velocity measurements and bending tests show that the freeze-thaw test places very minor demands on the samples from all seven localities.

-Evaluation of the results of the petrophysical investigations on samples from seven localities.

A summarized evaluation of all petrophysical investigations is difficult to make since, for example, in the freeze-thaw test, different rock characteristics are involved as in the acid test. A relative succession of the individual changes in the physical characteristics can be drawn up with the parameters recorded for each type of test. Samples which displayed little or no changes in reaction to the tests can definitely be graded as qualitatively higher than those samples which were altered. Samples IV and V, with their high carbonate content (cf. Tables 2 and 3) show much greater disintegration after the acid

test, both in the bending strength as well as in the reduction of the compression wave velocity (cf. fig. 13). However, this is not proportional to the carbonate content, but rather petrographic and structural characteristics also play a role, which thus led to the relatively better results obtained for sample V despite a high carbonate content. When considering the bending strength as a whole (Table 11), the structural characteristic of the angle between cleavage and stratification also plays a role. Thus, the only slate, where bedding and cleavage are in parallel (German: Massenschiefer) (cf. ARBEITSGRUPPE DACHSCHIEFER TRIER 1989, WAGNER 1994b) also has the best values, whilst the other slates (with a clear angle between cleavage and stratification, German: Druckschiefer) display lower values. In any case, the reduction in bending strength after the thermal cycle test and the freeze-thaw test is also the highest in this "Massenschiefer" (sample III).

5. Summary of the results as an impetus for a new European slate standard (EN 12326, Parts 1 and 2)

The sampling ought be to carried out in accordance with the DIN 52 101 standard. If possible, the sampling should occur in the extraction area itself.

Preparation of the samples must be carried out in a more precise manner than that recommended to date by the DIN standards. It makes sense to use a unified tile size of 200 mm by 100 mm for all experiments, and also a thickness, as unified as possible, of around 5 mm. Through this standardisation it is possible to conduct various petrophysical investigations in a row on the same tiles. Furthermore, it would also be wise to cut the tiles with the aid of a diamond-bladed saw. In doing so, a better level of reproducibility can be achieved. In general, the investigations should not be carried out on air dry tiles, since their water content cannot be precisely defined. The experiments are easier to reproduce if they are carried out on either water-saturated or dried samples.

The raw density should be determined in accordance with DIN 52 102, i.e. on individual pieces after the buoyancy method (VB 1).

Deviating from DIN 52103, it is better to carry out the water absorption on slate sizes of 200 mm by 100 mm and 5 mm thickness. It is sufficient to check the water absorption under atmospheric pressure.

The bending test should be carried out in accordance to DIN 52 112, with a centre load beam and defined load increases. The investigation result would then be given as the normalized bending strength (breaking load divided by tile thickness at breakage point). The tiles should be tested in a water-saturated state when bending strength is measured after another previously conducted petrophysical investigation. For bending tests made on tiles without prior investigation, ten of the tiles that are to be utilised should be saturated in water and ten tiles dried (at 110°C). The condition “air dry”, as defined to date in the existing standards leads to unnecessary variation in the results. For tiles displaying a δ line, the breaking loads could spread since this is highly dependent on the orientation of the load beam to the δ line. This effect can be seen, amongst others, in some of the Spanish slates.

Thermal cycle tests and freeze-thaw tests should be carried out in accordance to DIN 52 204 and/or DIN 52 104. The damage to the tiles as a result of the experiments can be measured by ultrasound wave velocity measurements, normal to the cleavage, both

before and after the tests on water satured slates. The absolute velocities (water coupling) and the velocity differences should be presented. After both tests (thermal cycle tests and freeze-thaw tests), a further bending test should be conducted. In certain conditions, it would be wise to determine the water absorption level of the tiles under atmospheric pressure before conducting the bending test. From experience, it is best in both cases (thermal cycle tests and freeze-thaw tests) to quantify the effects of the investigations on the tiles with ultrasound wave velocity measurements, bending tests and water absorption tests.

The acid test should, in most respects, be carried out in accordance to DIN 52 206. The most suitable tile size is, however, 200 mm by 100 mm by 5 mm (due to the arguments presented in Chapter 4.5, as unified a thickness as possible is particularly important in all acid tests). The tiles should be cut with diamond-bladed saws. The tiles to be tested are dried at 110°C instead of being air dry. In addition, the ultrasound wave velocities normal to the cleavage ought to be measured both before and after the acid test. Following the acid test, a bending test ought to be carried out on water-saturated tiles. If a petrophysical investigation is carried out following the above guidelines, then it is possible to ascertain the petrophysical quality of a roofing slate from a previously unknown deposit in relation to roofing slates which have already been examined. If the petrophysical characteristics of a slate from on-going production requires investigation, then, according to our opinion, it is possible to make a statement on the equivalent petrophysical quality of the slate from raw density and water absorption alone. In the case of significant changes in these parameters, additional investigation can be carried out following the above guidelines.

In the meantime, some of these observations, which have resulted from the diligent commitment to the research plan outlined within this report, could be incorporated into the European standard system. Thus, the EN 12326-2 could, for example, prescribe drying at 110°C instead of air-drying.

The introduction of measurement through compression wave velocity before and after experiments has, to date, been rejected despite a better result capability due to the fact that the appropriate equipment is not available throughout Europe for the process of material investigation.

The introduction of the petrographic analysis into the EN 12326, Part 2, proved itself to be a decisive step for the utilisation of the new European slate standard although this has not been fully endorsed in the important slate standards of the rest of Europe. The now standardised methodology correlates with the research methods as described in section 2. The EN 12326 standard assigns the task of identification to the field of petrography. This implies that petrography must clarify whether we are truly dealing with argillaceous slate (roofing slate in the true sense of the word) or with special cases such as, for example, slates with a high carbonate content (so-called carbonate slates) and also slates with a high degree of metamorphosis (for example, phyllitic slate) or simply rocks which can easily be split that are not slates at all. In addition, the origin of the slate should also be narrowed down through petrology and confirmed if necessary. Both of these latter tasks are a precondition for a proper evaluation of all technical test results, which are encompassed within the scope of the standard.

The petrographic results yielded within the scope of the research project also allow the possibility of quality judgements to be made. Regrettably, this has, to date, not been considered within the scope of the new European standard.

Literature

ARBEITSGRUPPE DACHSCHIEFER, TRIER (1989): Die gesteinskundliche Analyse von Dachschiefern (DIN 52 201 A). - Der Dachdeckermeister, 6-**89**, S. 14-24, Bochum.

BENTZ, A. & MARTINI, H. J. (1968): Lehrbuch der angewandten Geologie. II/1,S. 1226-1229, 3 Tab., (Enke) Stuttgart.

DIN 52 100 (1935): Prüfung von Naturstein - Richtlinien zur Prüfung und Auswahl von Naturstein. 5 S., (Beuth) Berlin.

DIN 52 101 Draft (1986): Prüfung von Naturstein - Probennahme. 20 S., (Beuth) Berlin.

DIN 52 102 (1988): Prüfung von Naturstein und Gesteinskörnungen - Bestimmung von Dichte, Trockenrohdichte, Dichtigkeitsgrad und Gesamtporosität. 10 S., (Beuth) Berlin.

DIN 52 103 (1988): Prüfung von Naturstein und Gesteinskörnungen - Bestimmung von Wasseraufnahme und Sättigungswert. 4 S., (Beuth) Berlin.

DIN 52 104 (1982): Prüfung von Naturstein - Frost-Tau-Wechsel-Versuch. 6 S., (Beuth) Berlin.

DIN 52 106 Draft (1992): Prüfung von Naturstein und Gesteinskörnungen - Untersuchungen zur Beurteilung der Verwitterungsbeständigkeit. 14 S., (Beuth) Berlin.

DIN 52 112 (1988): Prüfung von Naturstein - Biegeversuch. 3 S., (Beuth) Berlin.

DIN 52 201 (1985): Dachschiefer, Begriff, Prüfung. 3 S., (Beuth) Berlin.

DIN 52 204 (1985): Prüfverfahren für Dachschiefer - Temperaturwechselversuch. 2 S., (Beuth) Berlin.

DIN 52 206 (1975): Prüfung von Dachschiefer. - Säureversuch. 1 S., (Beuth) Berlin.

DITTMAR, U. (1996): Profilbilanzierung und Verformungsanalyse im südwestlichen Rheinischen Schiefergebirge. - Beringeria (Würzburger geowiss. Mitt.), **17**, 346 S., 85 Fig., 7 Tab., 15 Plates, 1 Enclosure, Würzburg

EUROPEAN STANDARD PREN 12326-1 (1999): Schiefer und andere Natursteinprodukte für Dachdeckungen und Außenwandbekleidung - Teil 1: Produktanforderungen. 15 S., (Beuth) Berlin.

EUROPEAN STANDARD PREN 12326-2 (1996): Schiefer und andere Natursteinprodukte für Dachdeckungen und Außenwandbekleidung - Teil 2: Prüfverfahren. 36 S., (Beuth) Berlin.

FRANKE, W. & DALLMEYER, D. & WEBER, K. (1995): Geodynamic Evolution. - In: DALLMEYER, D. & FRANKE, W. & WEBER, K. (Hrsg.): Pre-Permian Geology of Central and Western Europe, S. 579-593, (Springer) Berlin - Heidelberg - New York.

FRANKE, W. & MEISCHNER, D. & ONCKEN, O. (1996): Geologie eines passiven Plattenrandes: Devon und Unterkarbon im Rechtsrheinischen Schiefergebirge. - Exkursion der geol. Vereinigung, **3**, 74 S., 49 Figs., Gießen.

FRANKE, W. & ONCKEN, O. (1990): Geodynamic evolution of the North-Central-Variscides - a comic strip. - In: FREEMAN, R. & IESE, P. & MÜLLER, S. (Hrsg.): The European Geotraverse: Integrative Studies, S. 187-194, Strasbourg.

HEISS, K. & ZALLMANZIG, J. (1994): Schiefer - landschaftsprägend und denkmalgerecht. - Bautenschutz u. Bausanierung, 5 & 6/**94**, 4 S., 4 Figs., (Müller) Cologne.

HIRSCHWALD, J. (1911): Handbuch der bautechnischen Gesteinsprüfung. IX. Teil: Die Dachschiefer einschließlich der Tonschiefer im allgemeinen und ihre Prüfung. S. 592-904, Berlin.

HOPPEN, E. A. (1986/87): Schiefer, natürlicher Baustoff für Kenner und Könner. - Deutsches Dachdeckerhandwerk (DDH), Part 2: 22/**86**, S. 30-34, Part 3: 108. Jg, 1/**87**, S. 18-22, Cologne.

JUNG, D. (1994): Zur Frage der Qualitätsbeurteilung von Dachschiefer. - Schriftenreihe Schiefer-Fachverband in Deutschland e. V., **4**, s. 1-57, 35 Figs., Bonn.

KHORASANI, R. (1994): Einfluß von Karbonatgehalt und Gefügemerkmalen auf die Witterungsbeständigkeit von Dachschiefern, beschrieben an zwei Fallbeispielen mit Sauerländer Schiefer. - Schriftenreihe Schiefer-Fachverband in Deutschland e. V., **4**, S. 119-137, 14 Figs., Bonn.

KIRCHNER, K. & ZALLMANZIG, J. (1995): Lagerstättemkundliche Übersichtsuntersuchung und materialkundliche Charakterisierung der westfälischen Schiefergruben. - Metalla, **2/2**, S. 63-78, 9 Figs., 6 Tabs., Bochum.

KRAUTKRÄMER, J. & KRAUTKRÄMER, H. (1986): Werkstoffprüfung mit Ultraschall. 708 S., (Springer) Berlin - Heidelberg - New York - Tokyo.

NEGENDANK, J. F. W. & WAGNER, W. & BAUMANN, H. & ROSCHIG, F. (1991): Projekt Wirtschaftsnahe Forschung - Dachschiefer. Abschlußbericht: 161 S., 15 Figs., 27 Tabs., 3 Plates, Appendix A to H: 148 S., 52 Figs., 117 Tabs., University of Trier, Department of Geology, Trier (University publication).

ÖNORM B 3123 PART 1 (1990): Prüfung von Naturstein, Verwitterungsbeständigkeit, Beurteilungskriterien. 11 S., (O.N.), Vienna.

VAN RHIJN, J. C. & MELKERT, M. J. A. (1993): Petrographical Criteria for the examination of roof slates. Expertise, 74 S., (Rockview) Amsterdam.

WAGNER, W. (1992): Dachschiefer in der Lagerstätte. - Schriftenreihe Schiefer - Fachverband in Deutschland e.V., **1**, S. 75 -82, Bonn.

-W. (1994a): Geologische Vorgaben zur Gewinnung und zur Optimierung der Gesteinsausnutzung im Dachschieferbergbau. - Mainzer geowiss. Mitt., **23**, S. 39-50, 8 Figs., 1 Tab., Mainz.

-W. (1994b): Die Gesteinskundliche Analyse des Dachschiefers nach DIN 52 201 A. - Schriftenreihe: Schiefer-Fachverband in Deutschland e.V., **3**, S. 139-145, Bonn.

-W. (1996): Geologie und Europäische Normung - Erkenntnisse aus der normung von Schiefer, Natursteinen und Gesteinskörnungen. - Nachr. deutsch geol. Ges., **58**, S. 33 - 39, 3 Tabs., Hannover.

WAGNER, W. & HOPPEN, E. A. (1995): Forschungen zur Modernisierung des Schieferbergbaus. - Schriftenreihe GDMB, **73**, 333 S., 105 Figs., 7 Tabs., Clausthal-Zellerfeld.

WAGNER, W. & LE BAIL, R. & HACAR-RODRIGUEZ, M. & STANEK, S. (1995): European roofing slates, part 2: Geology of selected examples of slate deposits. - Z. angew. Geol., **41**, 1, S. 21 -26, 8 Figs., Stuttgart.

WAGNER, W. & STANEK, S. (1991): Loziska štipatelných jílouých bridlic v Europe se zvláštním zretelem na moravskolezský kulm. - Geologicky pruzkum, 5/**91**, S. 135 - 138, 3 Figs., 1 Tab., 1 Plate, Prague.

WEBER, K. (1976): Gefügeuntersuchungen an transversalgeschieferten Gesteinen aus dem östlichen Rheinischen Schiefergebirge (Ein Beitrag zur Genese der transversalen Schieferung). - Geol. Jb., D **15**, S. 3 - 98, Hannover.

Addresses of the Authors:

Dr. WOLFGANG WAGNER, Officially appointed and sworn expert for slate and slate mining, Im Nettetal 4, D-56727 Mayen, Germany.

Dr. HORST BAUMANN, Abt. Geologie, Universität Trier, D-54286 Trier, Germany.

Prof. Dr. JÖRG F. W. NEGENDANK, Direktor Aufgabenbereich 3: Struktur und Evolution der Lithosphäre, GeoForschungsZentrum Potsdam, Telegrafenberg 17 A, D14473 Potsdam, Germany.

Dr. FRANK ROSCHIG, Konrad-Adenauer-Str. 64, D-69207 Sandhausen, Germany.

Manuscript submitted on the 12.05.1997 and translated in March, 2000.

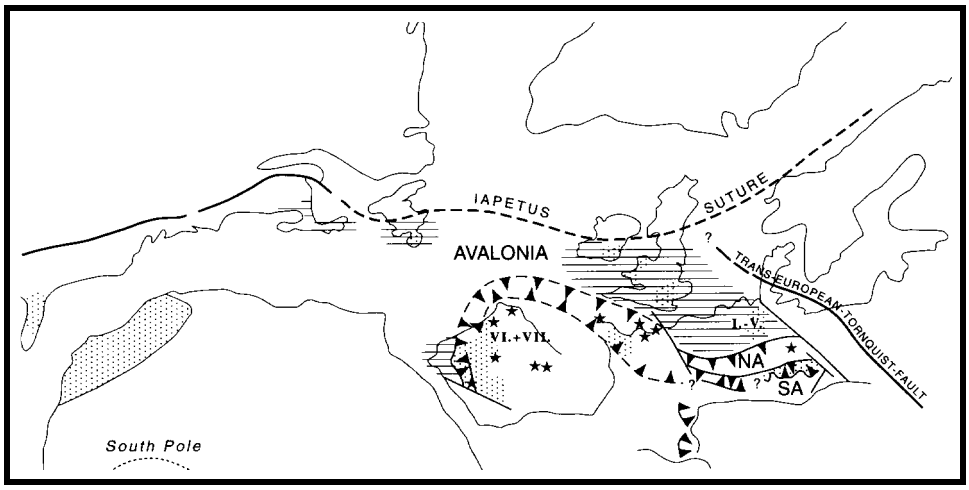

Fig. 1: Permic plate configuration with the deposit areas of samples 1 - VII. Dot pattern: Placement of the Cadomic basement; * = Traces of the Sahara glaciation; NA, SA: North and South Amorica (from FRANKE & MEISCHNER & ONCKEN 1996)

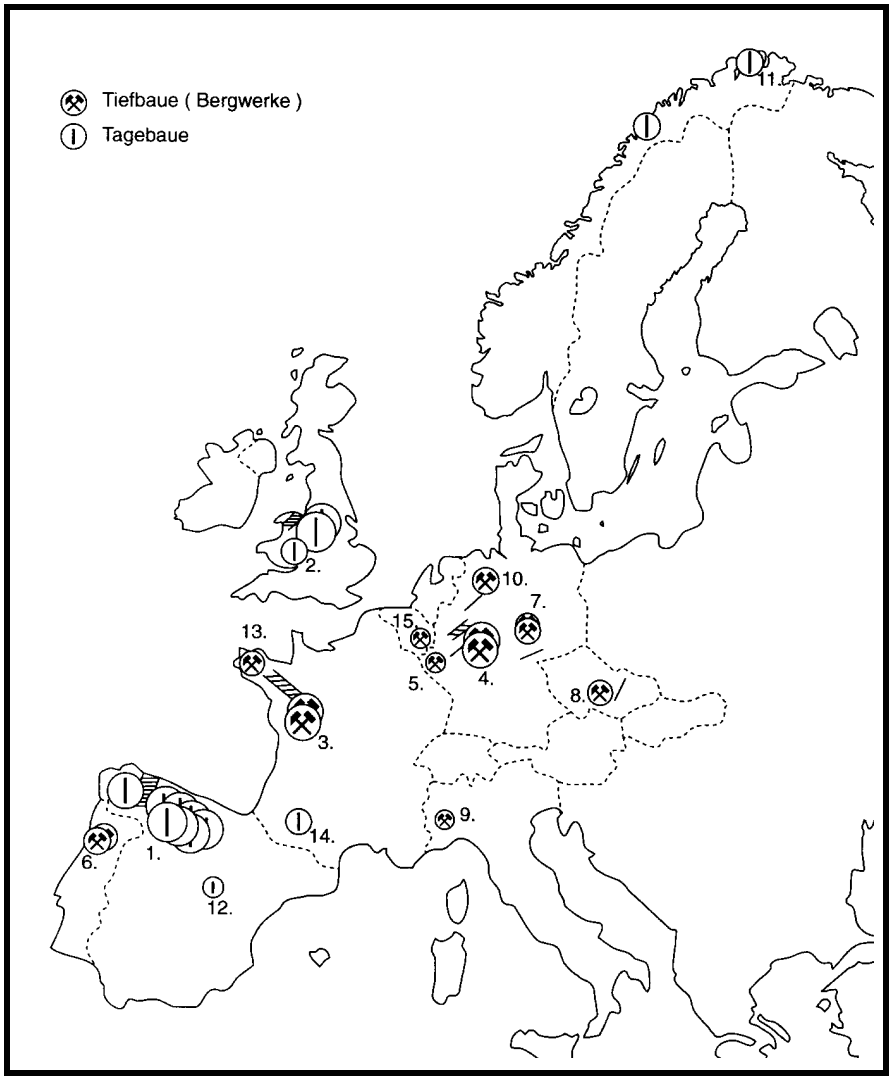

Fig. 2: Roofing slate extraction areas in Western Europe (numbering refers to occurrences referred to in the text).

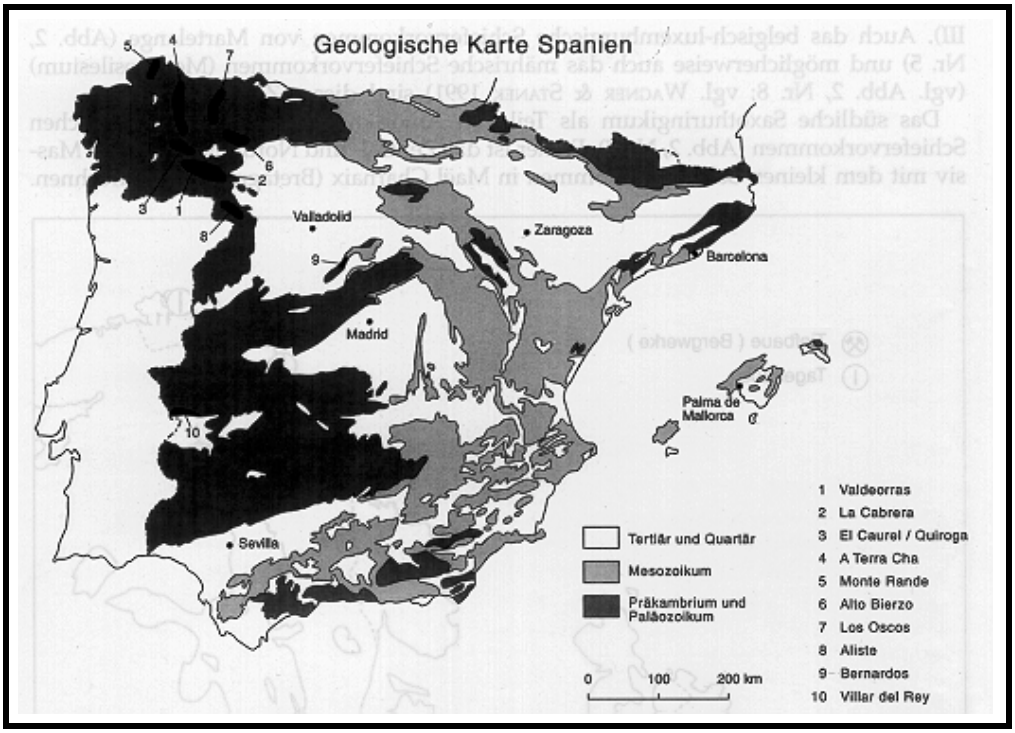

Fig. 3: Geological map of Spain with the most important roofing slate extraction zones.

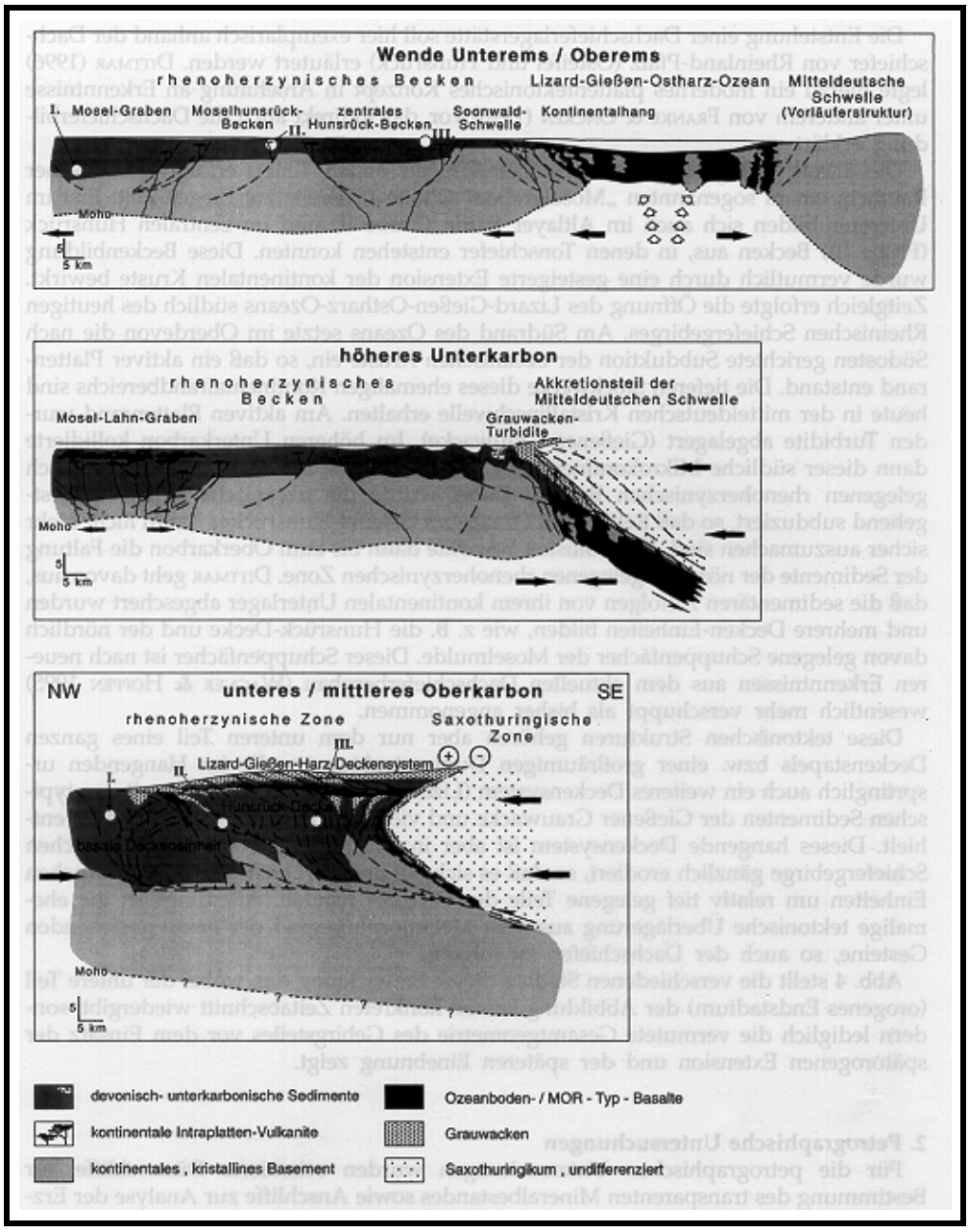

Fig. 4: Sketches of the geological development in the area of the occurrences of samples I, II and II (after DITTMAR 1996)

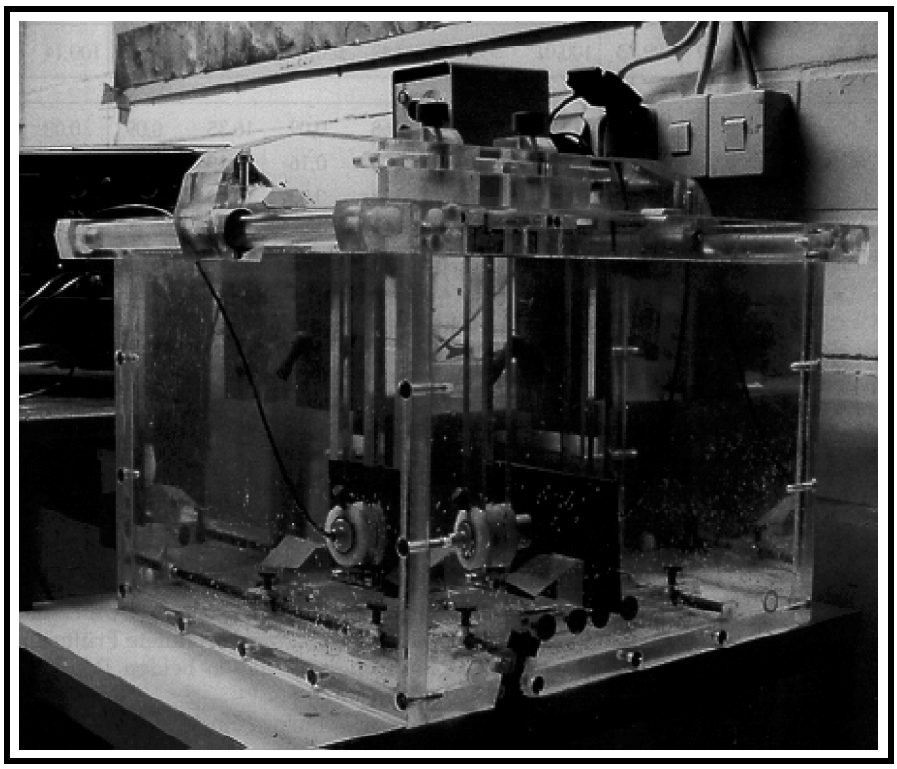

Fig. 5: Test device for the determination of ultrasound wave velocities with immersion coupling (constructed in our own laboratory)

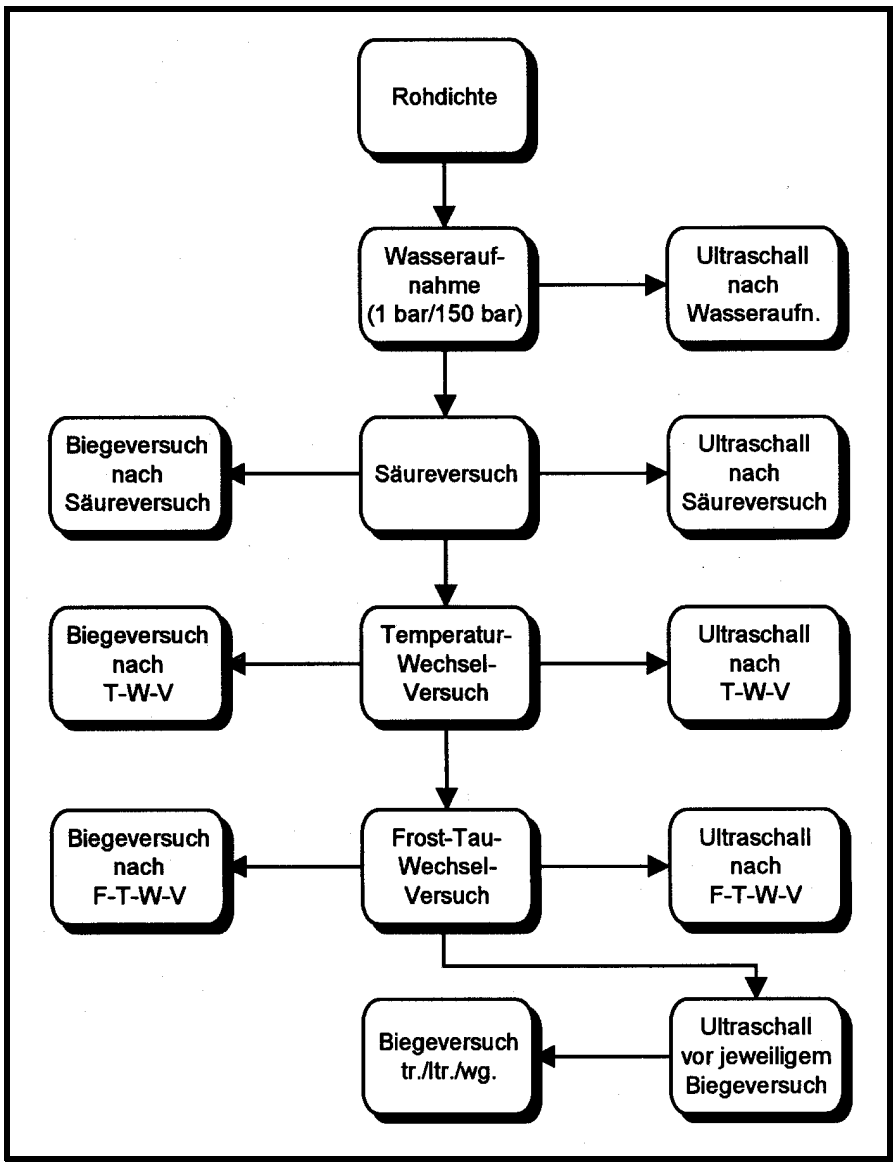

Fig. 6: Flow chart of the petrophysical processing of samples I to VII

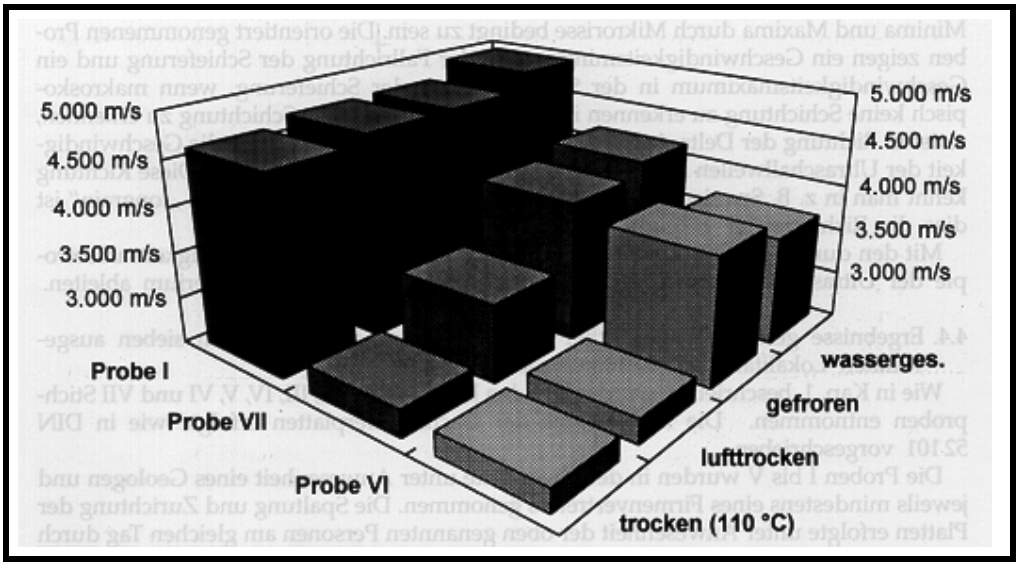

Fig. 7: Influence of the water content and/or the physical condition of the water on the ultrasound wave velocity for samples from sites I, VI, and VII.

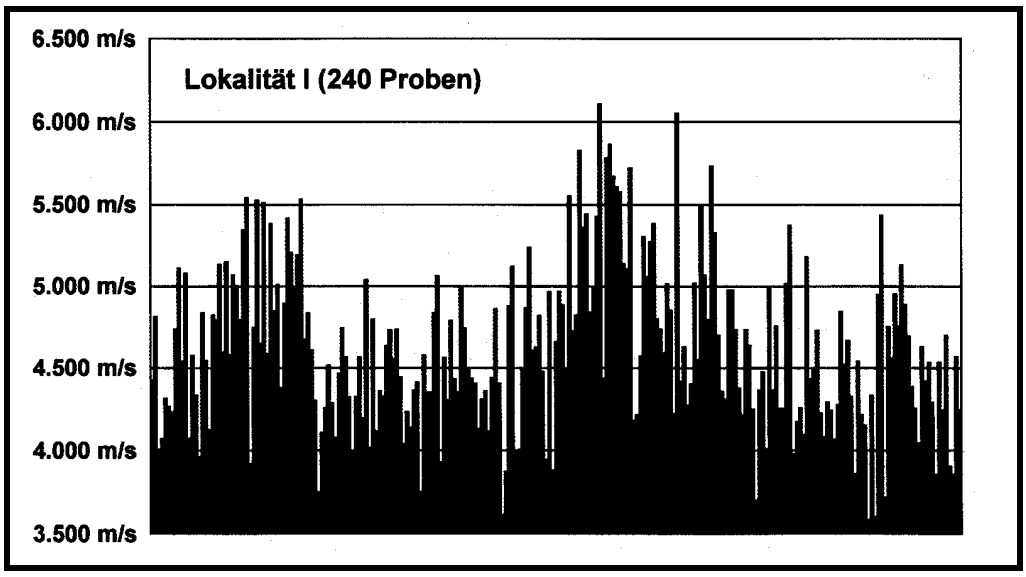

Fig. 8: Measured values of compression wave velocity on tiles from sample I (air dry). Dispersion of the wave velocity of slites from the same locality.

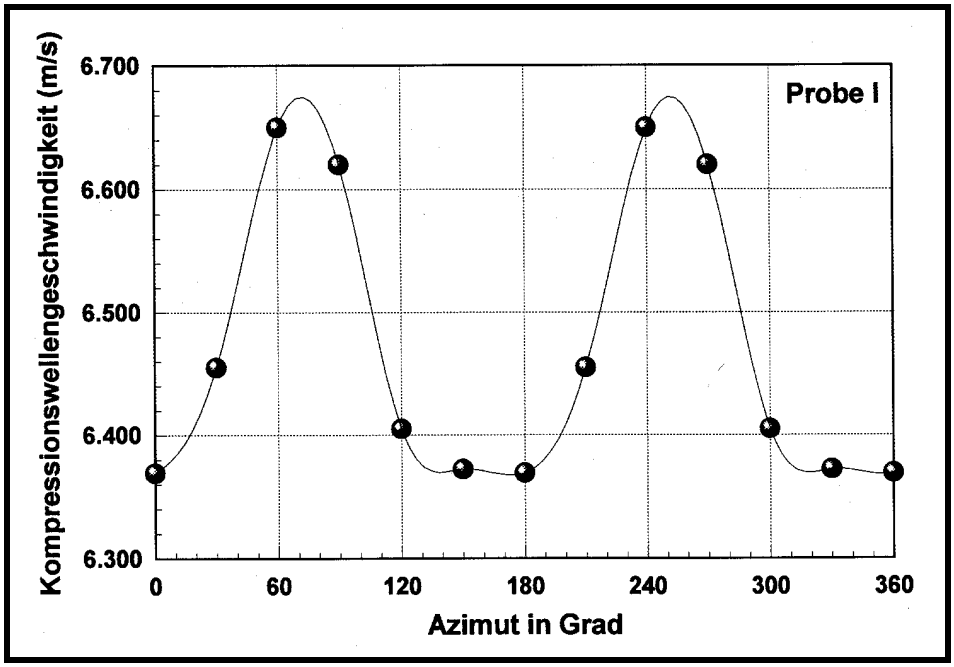

Fig. 9: Anisotropy of the ultrasound wave velocity of a cubic spline with a velocity maximum of 70° (250°), sample I.

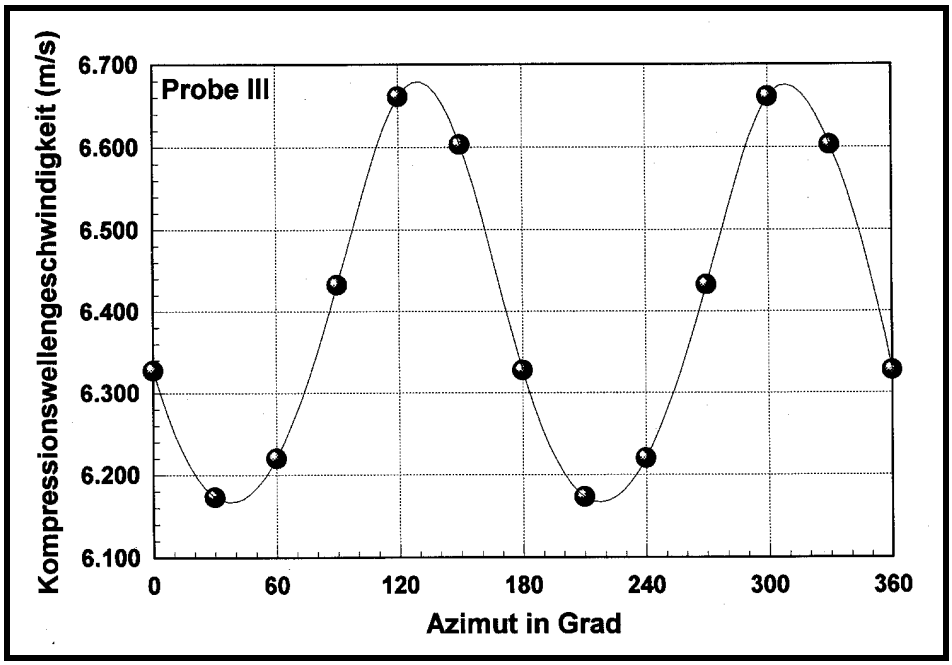

Fig. 10: Anisotropy of ultrasound wave velocity of a cubic spline with a velocity maximum of 130° (310°), sample III.

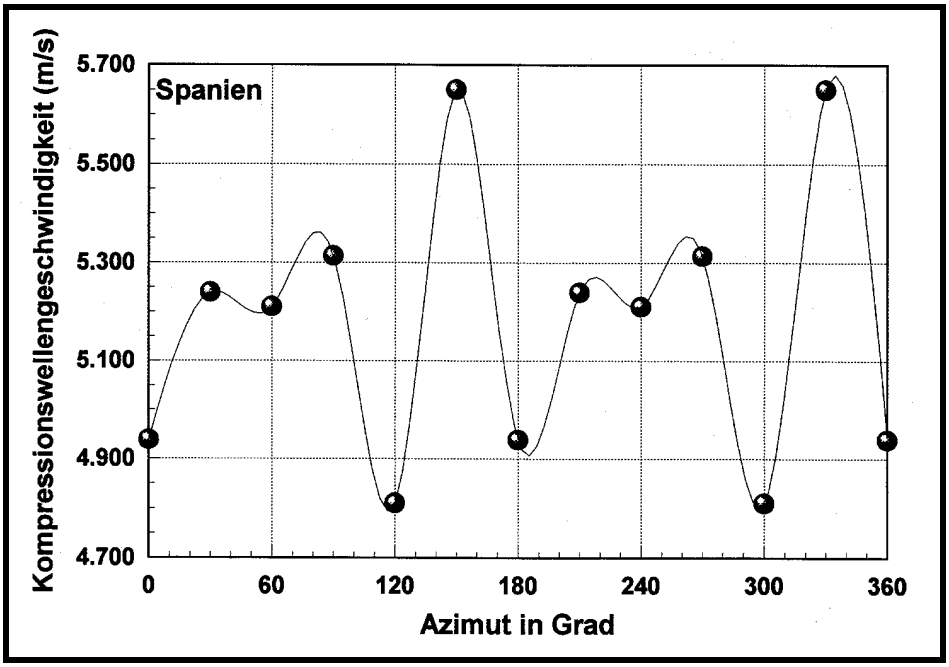

Fig. 11: Anisotropy of the ultrasound wave velocity of a cubic spline with three velocity maxima of 40°, 70°, and 150° (220°, 250°, and 330°), sample from Spain.

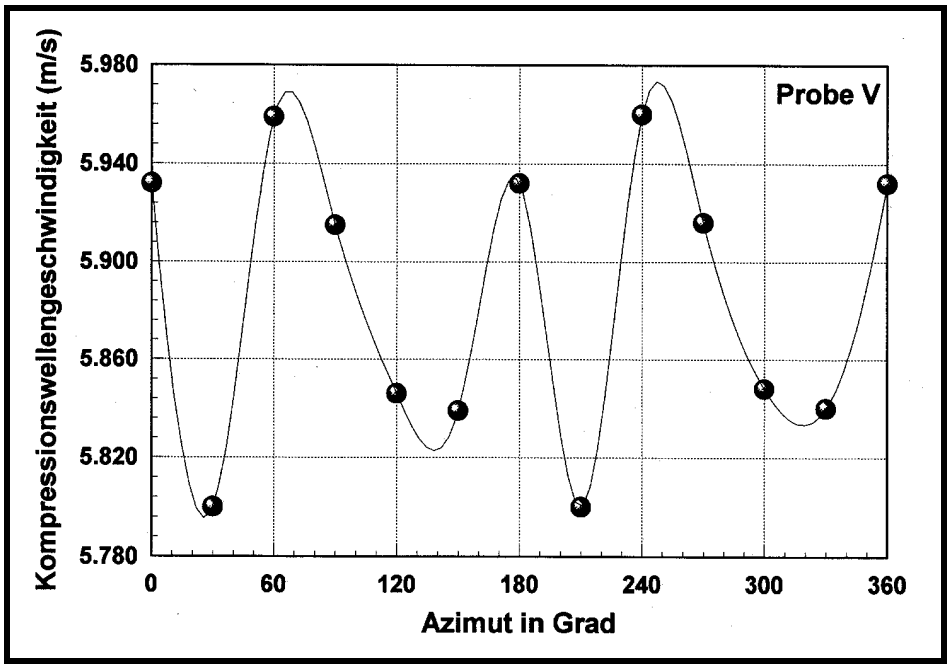

Fig. 12: Anisotropy of the ultrasound wave velocity of a cubic spline with two velocity maxima of 0°/360° and 70° (180°, 250°), sample V.

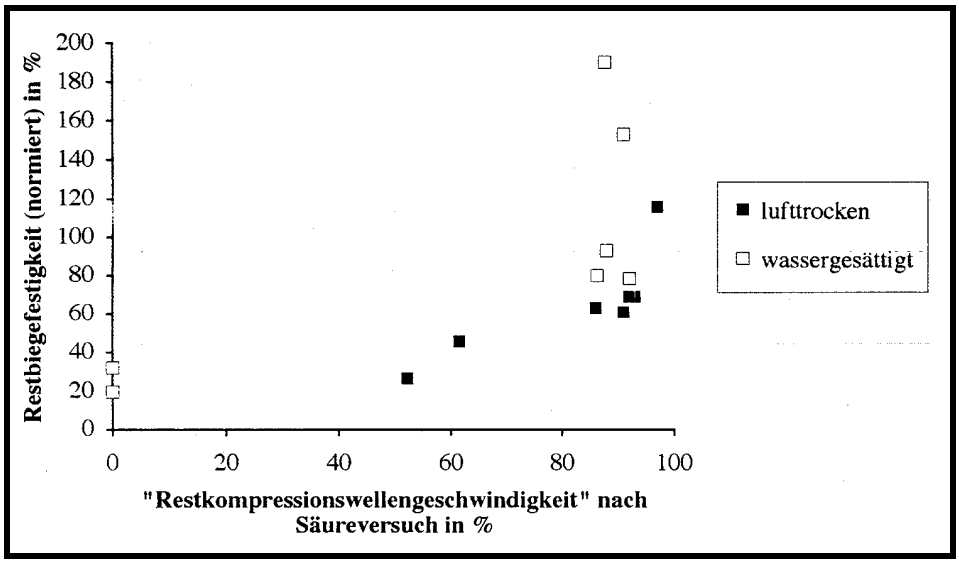

Fig. 13: Bending strength after the acid test in percent compared to the bending strength before the acid test (Y-axis). Compression wave velocity after the acid test in percent compared to the compression wave velocity before the acid test (X-axis).

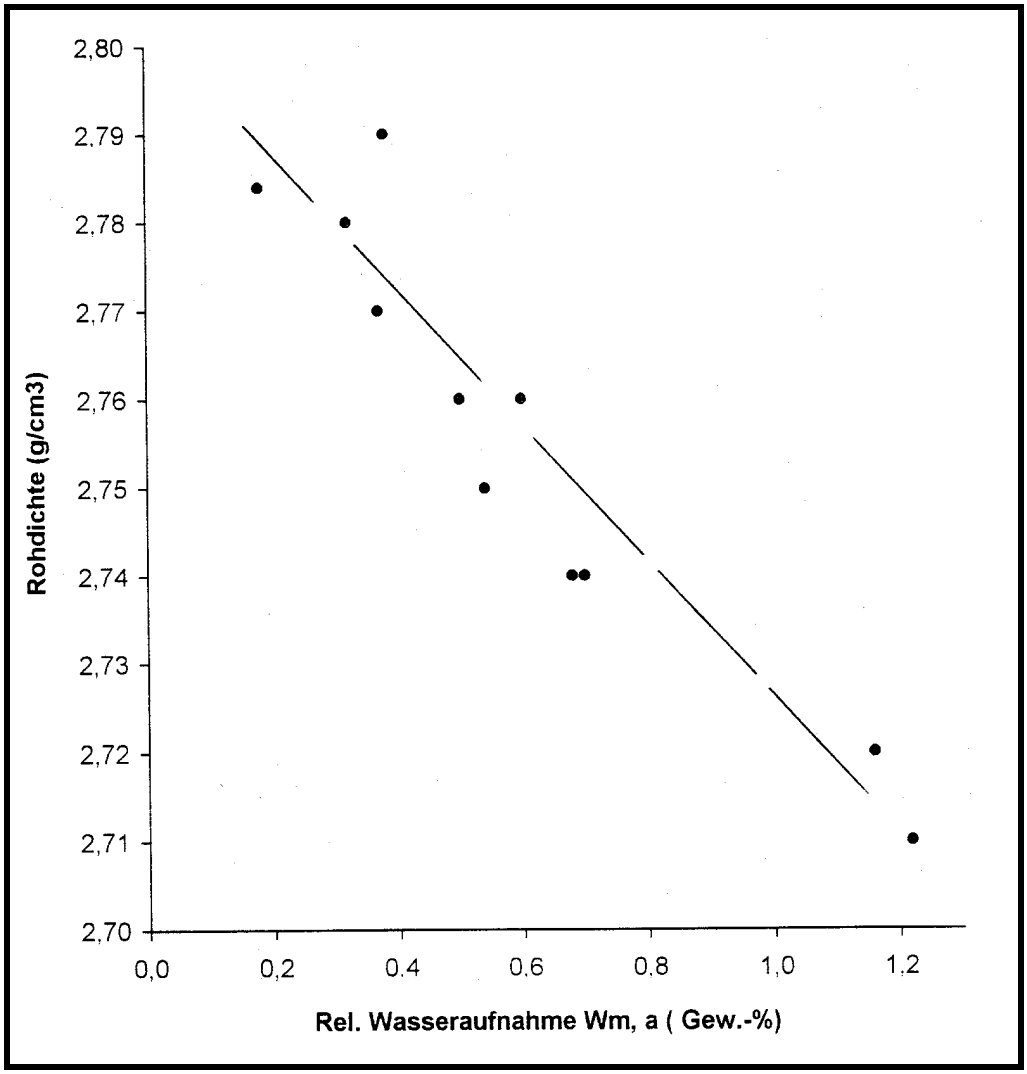

Fig. 14: Gross density of slates compared with water absortption.

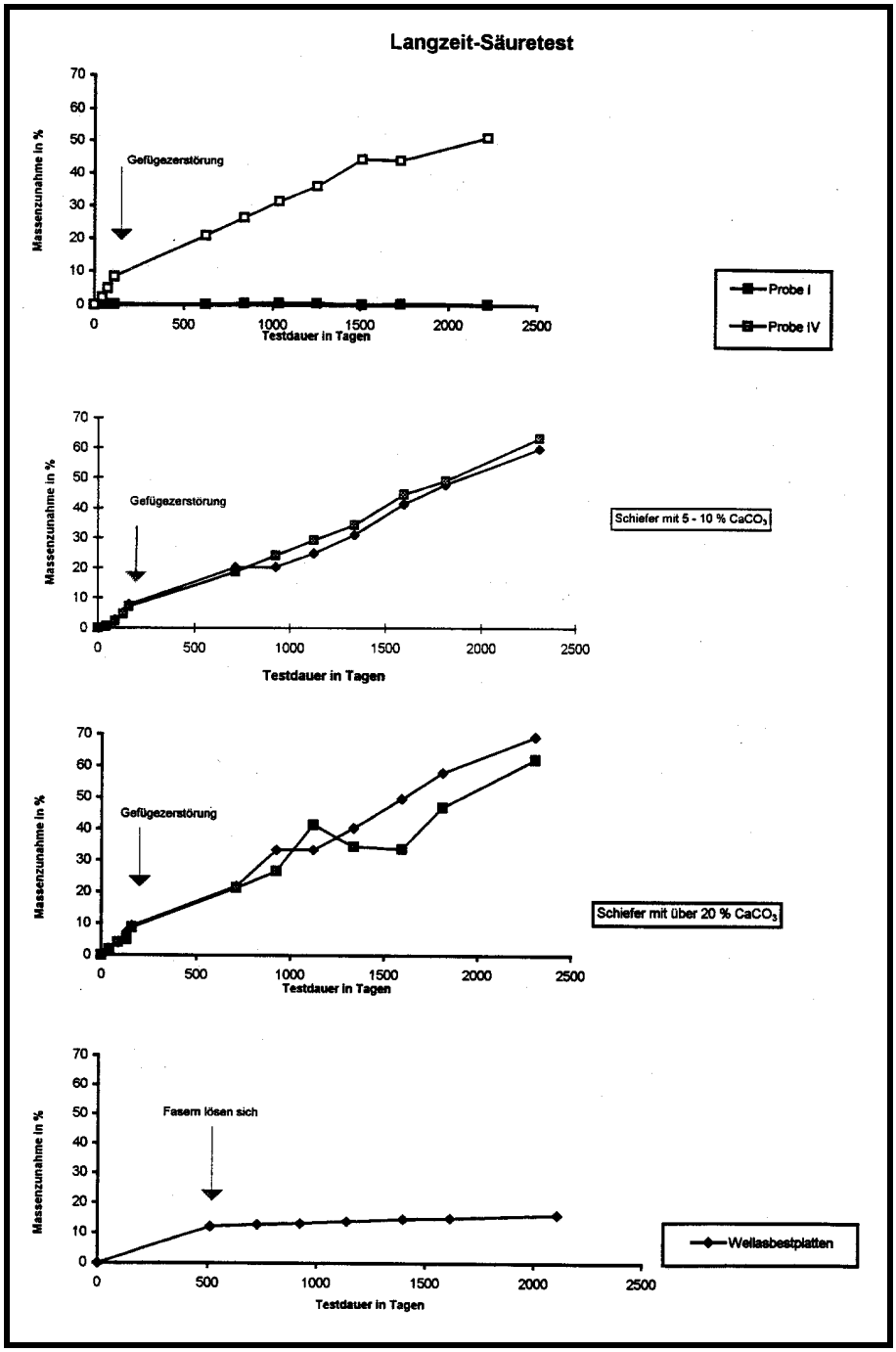

Fig. 15: Results of ”long time” acid tests of slates and ”Wellasbestplatten” (asbestos cement tiles).

Tab. 1: Petrographie und Gefüge der Proben der Reihenuntersuchung (Dünnschliffauswertung).

Lokalität	I	II	III	IV	V	VI	VII
Petrographische Beschreibung	Tonschiefer mit Siltlinsen	Tonschiefer mit Siltlinsen	Tonschiefer mit Siltlinsen	mergeliger Tonschiefer mit Siltlinsen	mergeliger Tonschiefer mit Silt-(Karbonat-)linsen	Tonschiefer	Phyllitschiefer
	P.: Quarz, Chlorit, (selten Karbonat)	P.: Chlorit z. T. Quarz (selten) Muskovit und Karbonat	P.: Quarz, Chlorit, (selten Karbonat)	P.: Quarz, Karbonat, Erz	P.: Quarz, Karbonat, Erz	P.: Quarz, Chlorit, Muskovit	P.: Karbonat, Quarzit, Quarz, Erz
	M.: Sericit, Chlorit	M.: Sericit, Chlorit	M.: Sericit, Chlorit	M.: Sericit, Chlorit	M.: Sericit, Chlorit	M.: Chlorit, Sericit	M.: Fe-Chlorit
Einzelproben	I,1, I,2, I,3, I,4, I,5	II,1, II,2, II,3, II,4, II,5	III,1, III,2, III,3, III,4, III,5	IV,1, IV,2, IV,3, IV,4, IV,5	V,1, V,2, V,3, V,4, V,5	VI,1, VI,2, VI,3, VI,4, VI,5	VII,1 VII,2, VII,3, VII,4, VII,5
Winkel sf/ss (Einzelmessungen)	5° 7° 10° 10° 11°	8° 8° 20°	//	// kl. 10° 12° 15°	8° ≈8° 7°	ø 15°	klein
Glimmerlagen/1 mm (Einzelwerte)	105 94 87 92 111	102 101 110 105 80	87 83 83 80 95	61 65 66 64 66	52 57 53 56 53	114 82 94 80 102	90 65 78 70 86
Glimmerlagen/1 mm (Durchschnitt)	**97,8**	**99,6**	**85,6**	**64,4**	**54,2**	**94,4**	**77,8**
Mengenwert (Durchschnitt)	2,8	4	4,1	1,3	1,2	2,6	6,4
Bemerkungen	I,3: Erzlinsen und Siltlagen I,4: Siltlinsen und Erzanreicherung	wenig Erze; Pyrit (Quadrate) in Nestern lagenförmig, z.T. Framboide II,4: häufig Pyrit	Schiefrigkeit oft undeutlich III,3: häufig Erznester, karbonatreiche Siltlagen III,5: dünne Erzlagen Wechselschichtung Ton-/Siltschiefer	IV, 2: Erznester IV,3: Erzanreicherung in Schichtung IV,4: großer Karbonat-porphyroblast (1 mm)	V,1: Porphyroblasten eckig, nicht eingeregelt	wenig Erze, Erzpigment	Erze (0,05–0,075 mm)

P = Porphyroblasten
M = Grundmasse

Tab. 2: Modaler Mineralbestand der Proben des Reihenversuchs (Angaben in Vol-%).

	I	II	III	IV	V	VI	VII	Beurteilung n. Van Rhijn & Melkert 1993 positiv		negativ	Richtwerte Bentz & Martini 1968
Sericit (inkl. Muskowit u. Paragonit)	41–51 %	43 %	42–47 %	41–42 %	36–37 %	44–50 %	46 %	größer 46 %	40–46 %	kleiner 40 %	um 40 % wichtig für Schieferung
Chlorit	19–20 %	23 %	22–26 %	17–18 %	15–16 %	25 %	17 %**				
Quarz	33–25 %	30 %	32–24 %	28–27 %	30–26 %	27–23 %	34 %*				um 30 % wichtig für Härte und Körnung
Karbonate	kleiner gleich 1 %	kleiner gleich 1 %	kleiner gleich 1 %	11–9 %	18–13 %	kleiner 1 %	1 %	kleiner 5 %	5–10 %	größer 10 %	bis 10 % Calcit
Rutil/Illmenit/ Titanomagnetit	2 %	2 %	2 %	1 %	1 %	2 %	2 %				
sonstige Erze	kleiner 1 %	kleiner 1 %	kleiner 1 %	kleiner 1 %	kleiner 1 %	1–2 %	kleiner 1 %				bis 4 % Pyrit
Sonstige	1 %	1 %	1 %	1 %	2 %	1 %	1 %				
Chlorit/Sericit-Verhältnis	0,37–0,48	0,54	0,50–0,55	0,41–0,45	0,41–0,45	0,50–0,58	0,37	kleiner 0,6	0,6–0,8		

* inkl. Feldspat
** insbes. Fe-Chlorit

Tab. 3: Chemische Analysen (Gew.-%) der Proben des Reihenversuchs.

	I,1	I,2	I,3	I,4	I,5	II	III,1	III,2	III,3	III,4	III,5	IV,1	IV,2	IV,3	IV,4	IV,5	V,1	V,2	V,3	V,4	V,5	VI,1	VI,2	VII
SiO_2	55,96	57,61	57,96	58,74	54,75	56,15	52,87	58,21	58,62	54,91	56,59	52,16	52,38	52,88	53,18	53,22	48,53	52,33	50,84	50,98	49,52	53,01	54,62	59,49
TiO_2	0,94	0,89	0,87	0,82	1,02	1,01	0,98	0,91	0,89	0,96	0,98	0,76	0,76	0,73	0,75	0,76	0,67	0,67	0,68	0,67	0,68	1,22	1,14	0,98
Al_2O_3	19,70	19,36	18,42	17,91	21,46	20,64	22,20	19,32	19,68	20,78	20,63	15,89	16,04	15,64	16,47	16,28	14,09	14,66	14,41	14,98	14,62	23,46	21,59	19,22
Fe_2O_3	1,29	1,91	1,75	1,42	1,76	0,80	2,98	1,14	1,52	1,49	1,74	1,70	1,63	1,47	1,78	1,66	1,69	1,71	2,02	1,74	1,69	0,95	1,83	2,14
FeO	5,89	5,41	5,73	5,87	5,44	6,55	5,98	6,22	5,99	6,18	6,00	4,71	4,66	4,70	4,64	4,77	4,60	4,16	3,98	4,02	4,20	7,24	6,78	4,64
MnO	0,14	0,13	0,17	0,17	0,12	0,15	0,13	0,19	0,14	0,19	0,14	0,08	0,08	0,08	0,07	0,08	0,08	0,07	0,08	0,07	0,08	0,07	0,07	0,05
MgO	2,65	2,67	2,84	2,79	2,65	2,73	2,86	2,74	2,73	2,84	2,78	3,38	3,12	3,38	3,46	3,44	3,11	3,09	3,15	3,12	3,14	2,92	2,80	3,14
CaO	1,12	1,01	1,36	1,38	0,86	0,67	0,61	0,0	0,55	0,81	0,53	6,28	6,57	6,66	5,78	6,15	11,03	8,31	9,49	8,55	10,35	0,40	0,37	0,47
Na_2O	1,16	1,17	1,13	1,11	1,14	0,82	0,99	1,16	1,18	1,11	1,14	0,99	0,99	0,99	0,94	1,00	0,85	0,85	0,87	0,85	0,85	1,33	1,24	2,02
K_2O	3,80	3,73	3,37	3,27	4,36	3,88	4,12	3,36	3,42	3,77	3,79	3,40	3,44	3,28	3,54	3,18	2,97	3,14	3,03	3,20	3,07	3,91	3,36	3,99
P_2O_5	0,14	0,18	0,18	0,15	0,16	0,10	0,24	0,15	0,13	0,11	0,13	0,15	0,12	0,13	0,12	0,11	0,12	0,12	0,11	0,10	0,11	0,27	0,24	0,12
GV 1050°	6,2	5,9	5,9	6,0	5,9	5,74	6,0	5,4	5,0	5,6	5,5	9,4	9,5	9,0	8,6	9,0	12,4	10,4	11,4	10,6	11,8	5,10	5,04	3,60
Σ	98,99	100,00	99,68	99,63	99,62	99,24	100,20	99,70	99,85	98,78	99,95	99,20	99,59	98,94	99,33	99,98	99,60	99,54	100,06	98,88	100,11	99,91	99,08	99,86
CaO	0,11	0,13	0,64	0,61	0,43	0,52	0,32	0,66	0,38	0,68	0,38	5,22	5,33	5,57	4,69	5,03	9,35	7,06	8,00	7,47	8,81	0,14	0,12	
$CaCO_3$	0,19	0,23	1,14	1,09	0,77	0,93	0,57	1,18	0,68	1,21	0,68	9,32	9,51	9,94	8,37	8,98	16,69	12,60	14,28	13,33	15,73	0,25	0,21	
MgO	0,31	0,26	0,34	0,39	0,34	0,24	0,13	0,28	0,16	0,27	0,16	0,33	0,32	0,33	0,31	0,31	0,46	0,35	0,41	0,35	0,43	0,12	0,07	
$MgCO_3$	0,65	0,54	0,71	0,82	0,71	0,50	0,27	0,59	0,33	0,56	0,33	0,69	0,67	0,69	0,65	0,65	0,96	0,73	0,86	0,73	0,90	0,25	0,15	

Tab. 4: Chemische Analysen (Gew.-%), Rheinland-Pfalz, Dachschiefer des Unterdevon.

	Osteifel												Mittelhunsrück		Mittelrhein	
SiO_2	53,39	41,69	57,60	60,08	56,85	58,22	57,58	59,80	56,16	57,39	56,96	58,04	60,06	57,37	58,21	59,37
TiO_2	1,06	1,18	0,96	0,87	0,92	0,93	0,95	0,86	0,94	0,90	0,98	0,81	0,92	1,01	0,97	1,01
Al_2O_3	21,60	28,54	18,98	18,16	20,20	19,70	19,0	17,74	20,10	19,70	20,40	18,40	19,00	20,57	18,89	20,67
Fe_2O_3	1,24	1,15	1,11	1,29	1,08	1,02	1,33	0,80	0,46	1,28	0,95	0,95	0,92	1,18	0,66	1,09
FeO	6,89	8,20	6,14	5,28	6,28	6,23	5,94	5,98	7,42	5,98	6,29	8,77	5,59	6,02	6,29	5,30
MnO	0,11	0,10	0,12	0,12	0,12	0,09	0,16	0,18	0,16	0,12	0,11	0,10	0,13	0,17	0,24	0,08
MgO	3,23	3,60	2,74	2,66	2,79	2,73	2,81	2,83	3,13	2,69	2,93	3,75	2,50	2,64	2,70	2,38
CaO	0,68	0,39	0,83	0,95	0,48	0,54	1,19	1,41	0,81	0,93	0,63	0,42	0,67	0,82	1,25	0,37
Na_2O	1,02	0,46	1,21	1,06	1,05	1,03	0,98	1,13	1,13	1,00	1,14	0,82	1,29	1,11	0,99	1,16
K_2O	3,96	5,71	3,38	3,43	3,91	3,88	3,54	3,15	3,42	3,66	3,82	2,66	3,45	2,89	3,13	3,98
P_2O_5	0,22	0,18	0,20	0,21	0,23	0,25	0,28	0,15	0,17	0,40	0,15	0,18	0,16	0,14	0,11	0,12
GV 1050°	5,81	7,04	5,51	5,21	5,14	5,01	5,56	5,65	5,27	4,96	5,01	4,82	4,55	5,04	5,61	4,57
Σ	99,21	98,81	98,81	99,35	99,05	99,66	99,32	99,68	99,17	99,01	99,37	99,72	99,24	99,96	99,11	100,1
CaO	0,52	0,22	0,62	0,87	0,35	0,43	0,95	0,78	0,46	0,68	0,36	0,15	0,48	0,45	0,92	0,28
$CaCO_3$	0,92	0,39	1,11	1,55	0,62	0,77	1,70	1,39	0,82	0,63	0,64	0,27	0,86	0,80	1,61	0,50
MgO	0,21	0,10	0,26	0,29	0,15	0,17	0,32	0,31	0,17	0,24	0,14	0,08	0,19	0,15	0,34	0,11
$MgCO_3$	0,44	0,21	0,54	0,61	0,31	0,36	0,66	0,65	0,36	1,10	0,29	0,17	0,40	0,31	0,71	0,23

Spurenelemente (ppm)

Zn	106	128	104	104	116	98	128	116
Ni	76	96	72	66	128	74	72	76
Cr	132	198	126	128	144	128	132	140
Pb	4	6	13	7	27	7	15	11
Ag	0,62	0,75	0,53	0,54	0,61	0,48	0,78	1,18

Tab. 5: Chemische Analysen (Gew.-%), sonstiges Deutschland, Dachschiefer des Mitteldevon und Unterkarbon.

	1			2		
SiO_2	53,62	53,18	19,82	62,36	62,12	62,80
TiO_2	0,81	0,77	0,68	1,00	0,91	0,90
Al_2O_3	15,78	16,11	14,07	19,36	18,44	17,98
Fe_2O_3	1,17	1,13	1,78	0,47	0,08	0,48
FeO	5,05	5,16	3,93	5,47	7,96	6,19
MnO	0,10	0,07	0,07	0,07	0,08	0,10
MgO	3,50	3,44	3,15	1,94	2,20	2,18
CaO	6,55	5,65	9,43	0,17	0,17	0,72
Na_2O	1,02	0,91	0,80	1,22	1,13	0,88
K_2O	3,16	3,60	3,13	3,41	2,75	2,82
P_2O_5	0,08	0,12	0,15	0,12	0,12	0,12
GV 1050 °C	9,36	9,28	12,38	4,46	3,90	4,88
Σ	100,20	99,72	99,39	100,05	99,86	100,05
CaO	6,16	5,47	8,73	0,07	0,06	0,41
$CaCO_3$	11,00	9,76	15,58	0,12	0,11	0,73
MgO	0,41	0,40	0,51	0,03	0,03	0,15
$MgCO_3$	0,86	0,84	1,13	0,06	0,06	0,31

1 = Mitteldevon, Sauerland, Nordrhein-Westfalen (vgl. Abb. 2, Nr. 10)
2 = Unterkarbon, Thüringen (vgl. Abb. 2, Nr. 7)

Tab. 6: Chemische Analysen (Gew.-%), Nordwest-Spanien/Provinz Orense, Valdeorras, Dachschiefer des Mittleren bis Oberen Ordovizium.

SiO_2	57,10	59,87	59,33	59,24	62,06	58,56	58,55	58,57	56,71	57,51	57,83	61,09	52,83	52,34	61,56
TiO_2	1,12	1,08	1,01	0,95	1,04	1,02	1,08	0,98	1,02	1,01	1,04	0,93	1,18	1,01	0,89
Al_2O_3	22,62	19,10	20,58	21,37	16,93	21,50	21,43	21,38	22,84	21,76	21,68	19,97	22,21	24,50	15,35
Fe_2O_3	1,45	0,81	1,29	0,91	0,96	1,02	1,43	1,27	1,65	2,14	0,58	0,99	0,87	0,85	0,69
FeO	5,13	6,13	5,18	5,62	5,84	5,47	5,56	5,84	5,39	5,20	6,52	5,49	7,60	7,85	5,38
MnO	0,04	0,05	0,04	0,05	0,09	0,04	0,04	0,05	0,04	0,04	0,07	0,04	0,09	0,09	0,12
MgO	1,72	2,19	1,72	1,75	2,27	1,73	1,81	1,85	1,60	1,67	1,97	1,62	2,96	2,22	1,90
CaO	0,18	0,45	0,15	0,18	0,94	0,11	0,22	0,16	0,14	0,11	0,16	0,32	0,47	0,29	3,09
Na_2O	0,93	1,66	0,71	0,74	1,64	0,64	0,65	0,71	0,65	0,63	1,08	0,79	1,49	1,22	1,61
K_2O	5,07	3,76	4,95	5,02	3,13	4,91	5,06	5,00	5,55	5,19	4,83	4,55	3,63	2,99	2,57
P_2O_5	0,11	0,16	0,14	0,11	0,34	0,11	0,25	0,12	0,11	0,13	0,12	0,25	0,29	0,15	0,20
GV 1050°	4,07	4,24	3,90	4,12	4,26	4,33	4,05	3,95	4,24	4,39	3,93	3,80	5,15	6,00	5,73
Σ	98,88	99,80	99,00	100,06	99,50	98,94	100,16	99,88	99,97	99,78	99,81	99,84	98,77	99,21	99,09
CaO	0,11	0,27	0,09	0,06	0,78	0,08	0,11	0,10	0,08	0,09	0,09	0,09	0,24	0,08	2,67
$CaCO_3$	0,20	0,48	0,16	0,11	1,39	0,14	0,20	0,18	0,14	0,16	0,16	0,16	0,42	0,14	4,77
MgO	0,04	0,07	0,04	0,05	0,08	0,03	0,04	0,03	0,03	0,04	0,03	0,01	0,06	0,13	0,11
$MgCO_3$	0,08	0,15	0,08	0,10	0,17	0,06	0,08	0,06	0,06	0,08	0,06	0,02	0,13	0,27	0,23
Spurenelemente (ppm)															
Zn	106	96	104		104	80	114	106	90	224	172	118	98		130
Ni	38	38	10		36	32	42	14	38	32	94	64	34		58
Cr	98	86	98		86	88	98	96	104	92	100	88	72		110
Pb	28	29	16		25	140	21	13	23	21	29	60	35		36
Ag	0,55	0,49	0,50		0,90	0,49	0,70	0,71	0,50	0,57	0,64	0,64	0,44		0,69

Tab. 7: Chemische Analysen (Gew.-%), sonstige Dachschiefer Spaniens.

	1	2		3	4			5		
SiO_2	58,79	51,95	55,79	58,41	49,32	56,86	60,60	60,244	66,68	60,03
TiO_2	1,02	1,29	1,21	1,09	1,14	1,01	0,92	1,03	0,86	0,86
Al_2O_3	21,10	23,43	21,41	21,76	25,10	22,50	17,51	18,78	15,01	16,89
Fe_2O_3	0,98	0,99	0,47	1,25	1,16	0,64	0,52	0,71	1,60	2,86
FeO	6,30	7,67	7,33	5,19	8,81	7,14	6,00	5,98	4,06	4,00
MnO	0,10	0,09	0,07	0,03	0,05	0,05	0,10	0,10	0,09	0,10
MgO	2,18	2,88	2,56	1,95	2,60	2,11	2,13	2,72	2,23	3,29
CaO	0,26	0,35	0,32	0,29	0,59	0,38	1,93	0,31	0,36	0,95
Na_2O	1,15	1,07	1,80	1,26	1,30	1,19	1,42	2,28	2,27	2,06
K_2O	4,05	4,51	3,13	3,59	3,44	3,07	2,97	3,62	2,96	3,48
P_2O_5	0,14	0,43	0,25	0,21	0,18	0,12	0,19	0,11	0,09	0,12
GV 1050 °C	3,93	5,27	4,23	4,71	6,40	4,98	5,00	3,22	2,80	5,00
Σ	100,00	99,93	98,87	100,01	100,09	100,05	99,29	99,10	99,01	99,64
CaO	0,09	0,08	0,08	0,16	0,29	0,16	1,73	0,11	0,16	0,67
$CaCO_3$	0,16	0,14	0,14	0,29	0,52	0,29	3,09	0,20	0,29	1,20
MgO	0,04	0,05	0,03	0,06	0,13	0,10	0,05	0,10	0,34	3,78
$MgCO_3$	0,08	0,10	0,06	0,13	0,27	0,21	0,10	0,21	0,71	7,91

Spurenelemente (ppm)

Zn	150	120	122
Ni	58	50	42
Cr	124	106	106
Pb	17	21	19
Ag	0,69	0,65	0,70

1 = Mittelordovizium, Los Oscos, Provinz Lugo/Oviedo (vgl. Abb. 3, Nr. 7)
2 = Mittel- bis Oberordovizium, La Cabrera, Provinz León (vgl. Abb. 3, Nr. 2)
3 = Mittelordovizium, Alto Bierzo, Provinz León (vgl. Abb. 3, Nr. 6)
4 = Mittelordovizium, El Caurel, Provinz Lugo/León (vgl. Abb .3, Nr. 3)
5 = Oberes Präkambrium bis Unterkambrium, Bernardos, Provinz Segovia/Zentral-Spanien (Quarzitphyllit) (vgl. Abb. 3, Nr. 9)

Tab. 8: Chemische Analysen (Gew.-%), sonstige Dachschiefer Europas.

	1	2	3		4				5	6	7	8		9
SiO_2	52,31	55,08	50,21	50,61	59,19	58,10	59,01	59,01	52,33	59,91	57,88	60,77	61,45	52,34
TiO_2	0,88	0,95	1,03	1,06	0,99	1,01	0,95	0,91	0,96	1,00	0,86	1,15	1,03	1,07
Al_2O_3	20,23	20,25	26,40	26,25	20,36	20,84	20,19	19,89	20,43	19,09	14,55	18,09	17,54	24,50
Fe_2O_3	14,86	1,03	1,97	1,67	8,19	8,34	7,47	8,47	1,92	2,07	4,39	1,63	1,20	0,61
FeO	1,30	6,22	6,96	7,31	0,79	0,63	0,94	1,11	6,82	2,72	2,34	5,06	5,40	7,41
MnO	0,50	0,22	0,08	0,08	0,19	0,18	0,24	0,24	0,12	0,08	0,17	0,10	0,10	0,10
MgO	1,50	3,34	2,00	1,96	2,17	2,16	2,29	2,29	3,47	2,67	2,09	2,26	2,32	2,13
CaO	0,34	1,51	0,23	0,24	0,85	0,86	0,75	0,74	1,26	1,11	5,67	0,82	0,76	0,77
Na_2O	1,15	0,89	1,17	1,19	2,07	1,99	1,90	2,04	0,89	2,68	3,12	2,25	2,59	0,93
K_2O	3,27	4,17	3,07	3,11	3,00	3,03	2,78	2,73	3,90	4,28	2,40	3,91	3,42	3,17
P_2O_5	0,18	0,14	0,15	0,16	0,10	0,09	0,08	0,08	0,19	0,12	0,11	0,20	0,10	0,19
GV 1050 °C	3,32	6,86	5,60	5,50	3,30	3,40	3,40	3,34	6,92	3,62	6,24	3,66	3,24	6,00
Σ	99,87	100,66	98,87	99,41	101,20	100,63	100,00	100,85	99,21	99,35	99,82	99,90	99,15	99,52
CaO	0,10	1,24	0,07	0,07	0,09	0,10	0,10	0,11	0,88	0,23	5,03	0,08	0,05	0,61
$CaCO_3$	0,18	2,21	0,12	0,12	0,16	0,18	0,18	0,20	1,57	0,41	8,98	0,14	0,09	1,09
MgO	0,08	0,55	0,17	0,16	0,03	0,04	0,03	0,04	0,42	0,12	0,08	0,11	0,05	0,23
$MgCO_3$	0,17	1,15	0,36	0,33	0,06	0,08	0,06	0,08	0,88	0,25	0,17	0,23	0,10	0,48

1 = Unterordovizium, Vielsalm, Ardennen, Belgien (vgl. Abb. 2, Nr. 5)
2 = Unterdevon, Martelange, Ardennen, Belgien (vgl. Abb. 2, Nr. 5)
3 = Mittelordovizium, Angers-Trélazé, Dep. Anjou, Frankreich (vgl. Abb. 2, Nr. 3)
4 = Kambrium, Penrhyn (purpur), Nord-Wales, Großbritannien (vgl. Abb. 2, Nr. 2)
5 = Unterdevon, Obermartelingen, Luxemburg (vgl. Abb. 2, Nr. 3)
6/7 = Eokambrium, Vestertana-Fjord (6 = grün, 7 = rot), Finnmark, Norwegen (vgl. Abb. 2, Nr. 11)
8 = Eokambrium, Friarfjord, Finnmark, Norwegen (vgl. Abb. 2, Nr. 11)
9 = Ordovizium, Valongo/Porto, Portugal (vgl. Abb. 2, Nr. 6)

Tab. 9: Chemische Analysen (Gew.-%), Dachschiefer aus Übersee.

	1	2	3						4	
SiO_2	65,45	63,55	32,37	35,49	66,39	59,68	39,66	63,91	64,14	49,53
TiO_2	1,04	0,87	0,37	0,65	0,77	0,76	0,53	0,80	0,75	0,52
Al_2O_3	23,42	16,43	6,86	10,62	14,08	18,91	11,23	17,56	17,42	14,21
Fe_2O_3	0,57	1,16	1,17	1,03	1,40	7,60	1,24	0,69	0,92	9,04
FeO	0,10	4,80	2,19	3,09	3,81	0,80	3,32	4,82	5,59	1,59
MnO	n.d.	0,08	0,05	0,07	0,05	0,02	0,09	0,11	0,05	0,19
MgO	0,22	3,10	11,13	2,85	2,57	1,92	3,32	2,26	2,27	4,33
CaO	0,07	0,61	17,63	21,57	1,77	0,10	17,84	0,28	0,39	4,54
Na_2O	1,11	2,19	0,62	0,85	1,79	0,09	1,00	1,31	2,15	0,21
K_2O	4,93	3,38	1,21	1,95	2,35	7,57	2,09	3,64	3,14	7,00
P_2O_5	0,05	0,14	0,14	0,10	0,23	0,11	0,24	0,12	0,21	0,08
GV 1050 °C	3,54	3,42	26,27	21,59	5,21	3,18	19,02	4,00	3,10	9,08
Σ	100,50	99,73	100,01	99,86	100,42	100,74	99,58	99,56	100,14	100,32
CaO	0,04	0,38	12,40	20,36	1,68	0,09	16,35	0,09	0,08	1,78
$CaCO_3$	0,07	0,68	22,13	36,34	3,00	0,16	29,19	0,16	0,14	3,18
MgO	0,02	0,05	5,26	0,89	0,38	0,03	0,43	0,05	0,04	0,95
$MgCO_3$	0,04	0,10	11,00	1,86	0,80	0,06	0,90	0,11	0,08	1,98

1 = Proterozoikum, Kanye, Botswana, Süd-Afrika
2 = Genauere Zuordnung unbekannt, Belo Horizonte, (graugrün) Minas Gerais, Brasilien
3 = Genauere Zuordnung unbekannt, China
4 = Genauere Zuordnung unbekannt, (Nord-) Indien

Tab. 10: Wasseraufnahme von Dachschiefern in Gew.-% und Rohdichten (Durchschnittswerte aus 10 Messungen).

Lokalität	**Wasser-aufnahme (1 bar) ohne Vorversuche (Wm, a)**	**Wasser-aufnahme 150 bar ohne Vorversuche (Wm, d)**	**Sättigungs-wert**	**Wasser-aufnahme (1 bar) nach FTW**	**Wasser-aufnahme 150bar nach FTW**	**Sättigungs-wert nach FTW**	**Rohdichte g/cm³**
I	0,32 %	0,33 %	0,97	0,38 %	0,35 %	1,09	2,78
II	0,60 %	0,61 %	0,98	–	–	–	2,76
III	0,38 %	0,38 %	1,00	–	–	–	2,79
IV	0,68 %	0,68 %	1,00	–	–	–	2,74
V	0,54 %	0,54 %	1,00	–	–	–	2,75
VI	1,11 %	1,22 %	0,91	1,24 %	1,32 %	0,94	2,72
VII	0,37 %	0,37 %	1,00	0,45 %	0,37 %	1,22	2,77
Richtwerte n. DIN 52100	ca. 0,5–0,6 %	–	–	–	–	–	ca. 2,7–2,8
Anforderungen n. DIN 52106 (für Werksteine)	< 0,5 %	–	–	–	–	–	–
	> 0,5 %	–	< 0,75	–	–	–	–
Anforderungen n. DIN prEN 12326-1	Code A1: < 0,6 % Code A2: > 0,6 % + FTW						

Tab. 11: Normierte Biegekraft von Dachschiefern in Newton und deren Veränderung nach gesteinsphysikalischen Versuchen (jeweils Durchschnitt aus mindestens 10 Versuchen).

Lokalität	**Biege-festigkeit in N/mm² (ltr.)**	**Normierte Biegekraft**					**Restf. nach SV in %**	**Restf. nach TW in %**	**Restf. nach FTW in %**
		tr. (110 °C)	ltr.	% von tr.	wg.	% von tr.			
I	(59,8)	114	(101)	88,60	76	66,7	(69,3 [ltr]) 93,4 (wg)	86,8 (wg)	(106,9 [ltr]) 97,4 (wg)
II	(58,1)	133	(102)	76,69	75	56,4	(62,7 [ltr]) 80,0 (wg)	90,7 (wg)	(89,3 [ltr])
III	(75,0)	188	(152)	80,85	111	59,0	(61,2 [ltr]) 78,4 (wg)	75,7 (wg)	(88,3 [ltr])
IV	(57,6)	143	(114)	79,72	78	54,6	(26,3 [ltr]) 32,1 (wg)	93,6 (wg)	(92,3 [ltr])
V	(49,5)	94	(99)	105,32	77	81,9	(45,5 [ltr]) 19,5 (wg)	76,6 (wg)	(87,0 [ltr])
VI	(29,7)	106	(57)	53,77	60	56,6	(116,0 [ltr]) 190,0 (wg)	79,7 (wg)	(161,4 [ltr])
VII	(36,6)	93	(61)	65,59	49	52,7	(68,9 [ltr]) 153,0 (wg)	74,5 (wg)	(126,2 [ltr])
Richtwerte nach DIN 52100 (z.T. umgerechnet)	(50–80)	–	(ca. 90–150)	–	–	–	–	–	–
Önorm B 3123-1	–	–	–	–	–	–	–	–	größer = 80 (tr)

tr = getrocknet 110 °C
ltr = lufttrocken
wg = wassergesättigt
SV = Säureversuch

Restf. = Restfestigkeit (nach Säureversuch, TW und FTW jeweils bezogen auf den vergleichbaren Zustand vor dem Versuch; tr, ltr oder wg)
TW = Temperaturwechselversuch
FTW = Frost-Tau-Wechselversuch
( ) = lufttrockene Werte sind für Vergleichszwecke ungeeignet (vgl. Text)

Tab. 12: Kompressionswellengeschwindigkeit und deren Veränderung in % nach Säureversuch, TW und FTW (Durchschnittswerte aus jeweils 5 Messungen).

Lokalität	vp (m)				Säureversuch				Temperaturwechselversuch				FTW I			Abnahme in %	FTW II			Abnahme in %
	tr	ltr	wg	gef	vor	nach	Diff.	Abnahme in %	vor	nach	Diff.	Abnahme in %	vor	nach	Diff.		vor	nach	Diff.	
I	4584	(4699)	4912	4736	(4414 [ltr]) 4150 (wg)	(4107 [ltr]) 3628 (wg)	(−307) −512	(6,96) 7,52	(4581 [ltr])	(4355 [ltr]) (35 TW)	(−226)	(4,93)	5066 (wg) (25 fTW)	4557 (wg)	−499	9,87	(4567 [ltr]) (50 FTW)	(4118 [ltr])	(−499)	(10,93)
II			3962		(3800 [ltr]) 3858 (wg)	(3262 [ltr]) 3332 (wg)	(−537) −526	(14,13) 13,63	4214 (wg)	4090 (wg) (25 TW)	−124	(2,94)	3815 (wg)	3709 (wg)	−106	2,78				
III			4727		(4190 [ltr]) 4395 (wg)	(3800 [ltr]) 4048 (wg)	(−390) −390	(9,31) 8,87	4024 (wg)	3769 (wg) (25 TW)	−255	6,34	4128 (wg)	4114 (wg)	−14	0,34				
IV			4490		(4092 [ltr]) 4210 (wg)	(2130 [ltr]) –	(−1962) −4210	(47,95) 100,00	4048 (wg)	3934 (wg) (25 TW)	−114	0,03	4096 (wg)	4062 (wg)	−94	2,29				
V			4554		(4148 [ltr]) 4230 (wg)	(2552 [ltr]) –	(−1596) −4230	(38,48) 100,00	3946 (wg)	3873 (wg) (25 TW)	−43	1,09	3993 (wg)	4000 (wg)	+7	0				
VI	2686	(2711)	3631	3858	(3640 [ltr]) 3983 (wg)	(3543 [ltr]) 3494 (wg)	(−97) −489	(2,66) 12,50	(3412 [ltr])	(2998 [ltr]) (35 TW)	(−414)	(12,13)	4191 (wg)	3676 (wg)	−378	12,29	3476 (wg)	3098 (wg)	−378	10,87
VII	2749	(3309)	4148	3978	(4162 [ltr]) 4444 (wg)	(3845 [ltr]) 4062 (wg)	(−317) −382	(7,62) 8,60	(2958 [ltr])	(2780 [ltr]) (35 TW)	(−178)	6,02	4756 (wg)	4389 (wg)	−447	7,72	4742 (wg)	4295 (wg)	−447	9,43

gef. = gefrorene Probe

() = lufttrockene Werte sind für Vergleichszwecke ungeeignet (vgl. Text, weitere Abkürzungen s. Tab. 11)